Characterizing the Marine Energy Test Area (META) in Wales, UK

Neill, Simon; Fairley, Ian; Rowlands, Steven; Young, Saul; Hill, Tom; Unsworth, Christopher; King, Nicholas; Roberts, Michael; Austin, Martin; Hughes, Peter; Masters, Ian; Owen, Aled; Powell, Ben; Reeve, Dominic E.; Lewis, Matthew

Renewable Energy

DOI:
10.1016/j.renene.2023.01.105

Published: 01/03/2023

Peer reviewed version

Characterizing the Marine Energy Test Area (META) in Wales, UK

Simon P. Neill[a,*], Iain A. Fairley[b], Steven Rowlands[a], Saul Young[c], Tom Hill[c], Christopher A. Unsworth[a], Nicholas King[b], Michael J. Roberts[a], Martin J. Austin[a], Peter Hughes[a], Ian Masters[b], Aled Owen[a], Ben Powell[a], Dominic Reeve[b], Matthew J. Lewis[a]

[a] *School of Ocean Sciences, Bangor University, Menai Bridge, LL59 5AB, UK*
[b] *Faculty of Science and Engineering, Swansea University, Swansea, SA1 8EN, UK*
[c] *Marine Energy Wales, Pier House, Pembroke Dock, SA72 6TR, UK*

Abstract

With lack of convergence on any single wave or tidal technology, test centres have a unique role in the marine renewable energy industry. Test centres facilitate real testing at sea for devices and components at various TRLs (Technology Readiness Level), reducing the time, cost, and risks faced by marine energy developers. META (Marine Energy Test Area) is a £2.7M project managed by Marine Energy Wales (MEW), consisting of eight test areas in the Milford Haven Waterway and surrounding waters (Pembrokeshire, Wales). Although various datasets have been collected from the META test areas over the last decade, and some aspects of these data have been published in various reports, the data has not been gathered together, systematically analyzed and critically assessed – the aim of this study. Here, we describe and interpret the various META datasets, including multibeam, ADCP (acoustic Doppler current profiler), and wave buoy data. We report the key parameters of relevance to testing at META, including bathymetry, the nature and magnitude of the tidal currents, turbulence, and wave climates. We make recommendations on future priorities for data collection at META, and discuss the future of the test areas, including expansion into floating wind and other evolving marine energy technologies.

Keywords: Tidal energy, Wave energy, Acoustic Doppler Current Profiler, Wave buoy, Multibeam echosounder, Turbulence

*Corresponding author
Email address: s.p.neill@bangor.ac.uk (Simon P. Neill)

1. Introduction

Since EMEC (European Marine Energy Centre) was established in 2003, ocean renewable energy test centres have assumed an important role in the evolution of the industry [1]. Ocean energy test centres provide facilities where either smaller scaled devices, or devices that are at early stages of development, can be tested in relatively sheltered real sea conditions, representing the next steps in technology progression following tank testing [2]. They can also offer facilities where larger prototypes can be tested in more energetic conditions, but in pre-consented, and often grid-connected, locations [3]. So far, 12 wave and 15 tidal energy developers have tested their technologies at EMEC, and other test centres have emerged around the world, including FORCE (Fundy Ocean Research Centre for Energy) in Canada, and PMEC (Pacific Marine Energy Centre) in the USA [1]. Although a number of commercial projects are under development in the UK, and test facilities beyond EMEC have been created (e.g. WaveHub and FabTest), the formation of META (Marine Energy Test Area) in Pembrokeshire (Wales) complements these existing facilities.

META is a £2.7M project managed by Marine Energy Wales (MEW). META consists of eight pre-consented test areas in the Milford Haven Waterway and surrounding waters (Fig. 1), providing the opportunity to test devices, sub-assemblies and components. The mission of META is to reduce the time, cost and risks faced by marine energy developers in order to accelerate growth in the sector, whilst complementing the existing test centre network across the UK. Due to the diversity of the marine renewable energy resource and energy markets (e.g. high demand, grid-connected nations, or remote "off-grid" industries), there is no convergent marine energy technology design [4]. Therefore, META will greatly enhance the range of marine renewable energy technologies that can be tested.

META is easily accessible and therefore ideal for early stage developers, and is also a suitable base for research and innovation. Targeting Technology Readiness Level (TRL) $4-6$, the META sites are non-grid connected, ranging from sheltered port-based to open sea, yet accessible, locations. META is part funded by the European Regional Development Fund (ERDF, administered through the Welsh Government), the Coastal Communities Fund, and the Swansea Bay City Deal[1], and contributes towards plans for Wales to play

[1] An investment of up to £1.3 billion in a portfolio of major programmes and projects

a key role in a growing global marine renewable energy market. META is well positioned to act as a stepping stone towards full scale deployment at the two offshore demonstration zones in Wales: the North Wales tidal stream demonstration zone [5] and the Pembrokeshire Demonstration Zone (PDZ) [6] for wave and floating wind (South Wales).

Over the last decade, various university-led projects have collected data across META to understand and characterize the sites. It is timely to now assess and publish these datasets, including critical analysis and interpretation, to characterize the sites in more detail, and to inform future data collection and testing at META.

2. Background to META

META was conceived by Marine Energy Wales to bridge the gap between tank testing and full scale demonstration. META secured funding in 2017 from the European Regional Development Fund, ERDF (administered through the Welsh European Funding Office, WEFO). This funding initiated the complex licensing and leasing process required to consent the broad design envelope required to install and test a range of novel marine energy technologies, including wave and tidal energy converters. During this process, technology developers participated in surveys to understand their testing requirements, and test sites were identified to meet their current and future needs. The sites were categorized into *Quayside* and *Open Water* (Table 1), with the two categories requiring different levels of consents.

The Quayside sites followed a simpler licensing process and were awarded the relevant consents to become operational in September 2019, leading to the first technology trials in 2021 of a novel tidal stream measurement device. The Open Water sites required an Environmental Impact Assessment to be submitted to the marine licensing regulatory body (Natural Resources Wales, NRW). The marine licence for these sites was awarded in January 2021, followed by the Crown Estate Lease in August 2021, making the test centre fully operational, with the first experimental device deployed in November 2021. Most of the sites are within the jurisdiction of the Port of Milford Haven, which contains a LNG terminal and hosts a significant number of recreational users. Navigational risk assessment is carried out in dialogue

across the Swansea Bay City Region.

with the port. The first deployment at the Open Water sites was a larger scale version of the novel tidal stream measurement device at Warrior Way. The second was a multi-use test buoy used to test floating solar, marine coatings, and a new mooring damper system. Meanwhile, the first full scale generating device will be Bombora Wavepower's mWave at East Pickard Bay, planned for deployment in Autumn 2022. A further £783,000 of funding was secured for the project from the Swansea Bay City Deal in 2020, ensuring the continual operation and development of the test centre until at least 2025.

3. META data collection

For wave and tidal stream projects, the key dynamical properties to be gathered are those that relate to the power matrices [7] or power curves [8] of wave and tidal energy converters, respectively. Interpolation of the power matrix/curve allows the instantaneous power output for specific devices to be calculated (the technical resource), and so variables such as annual energy yield and capacity factor can be determined [8]. These key variables are significant wave height, wave period (generally the energy wave period), and depth-averaged and depth-varying current speeds. It is also common, while collecting current data, to simultaneously collect data on turbulence, as this affects device performance and loading [9, 10]. In addition, accurate sea bed surveys, particularly those obtained using multibeam echosounders, allow water depths to be determined at each possible device location, highlighting sea bed features that might affect device deployment. Multibeam surveys are usually accompanied by a study of temporal variations in water level so that the water depths under spring and neap conditions can be calculated – this is particularly relevant for devices that would be fixed to the sea bed, since there could be large variations in water depth compared to the mean sea level.

3.1. Multibeam echosounder surveys

SEACAMS I, II (Sustainable Expansion of the Applied Coastal and Marine Sectors) was a £50M European Regional Development Fund (ERDF) programme delivered jointly by Bangor University and Swansea University between 2010 and 2022. The main aim of SEACAMS was to support the development and growth of businesses associated with the marine renew-

able energy sector in Wales through the delivery of collaborative RD&I[2] projects. As part of several such projects and the META initiative, numerous multibeam echosounder (MBES) surveys of the Milford Haven Waterway and surrounding areas were conducted in 2013 and 2017. Data was acquired using a frame-mounted SeaBat 7101 multibeam system deployed through a 'moon-pool' situated on the rear deck of a 7.9 m Cheetah catamaran survey vessel. The MBES system was coupled to an Applanix Wavemaster POS MV position and data recorder and dual Trimble DGPS receiver system to account for lateral and vertical movement of the vessel. Surface and water column sound velocity values were obtained using Reson SVP71 and SVP15T profilers, respectively. Tidal adjustment was applied from recorded vertical movement of the vessel. Data were collected using a frequency of 240 kHz, and the raw multibeam data was processed using the Teledyne PDS2000 software package. These data were subsequently corrected for changes in tidal height, water column sound speed, and lateral positioning. Positional data was referenced in the geographical coordinate system WGS84 and projected in Universal Trans Mercator (UTM) Zone 30N. All vertical elevations were reduced to mean sea level (MSL). Following these corrections, the data were exported and converted to a QPS Fledermaus bathymetric file type for detailed analysis and visualization. Although the resolution of a multibeam survey is dependent on vessel speed and water depth, typical resolutions achieved from the surveys in Milford Haven ranged from 0.2 to 0.5 m. Approximately 52 km^2 of seabed in the Milford Haven area was surveyed during two MBES survey programmes in 2013 and 2017, with each survey period typically taking $5 - 10$ days to complete.

3.2. Tide gauge data

The UK National Tide Gauge Network, owned and operated by the Environment Agency, records tidal elevations at over 40 locations around the UK coast. One of these locations is Milford Haven where a (bubbler[3]) tide gauge is installed at the seaward end of a concrete jetty (51°42.44′N 05°03.09′W). The data is available from 1953 to present. The time step is 15 minutes from September 1992 to present; older data is at a time step of 1 hour.

[2]Research, Development and Innovation.

[3]Also known as a gas purged pressure gauge – a type of water level gauge in which gas is emitted from a submerged orifice at a constant rate. Fluctuations in hydrostatic pressure due to changes in water level modify the recorded emission rate.

3.3. ADCP moorings

3.3.1. Mean flow properties

The SEACAMS project collected ADCP (acoustic Doppler current profiler) data in 2021 to assist Marine Energy Wales in characterizing META. The ADCP deployments at Warrior Way West and Criterion Jetty covered three spring-neap cycles (23 March – 10 May 2021), with the later Warrior Way East deployment (22 April – 10 May 2021) adding an extra datapoint at the Warrior Way test site (Table 2). The 500 kHz Nortek signature ADCPs at Warrior Way were deployed with 1 m bin size, and recorded at a frequency of 4 Hz. The RDI sentinel at Criterion Jetty has a slightly higher acoustic frequency (614 kHz), allowing for 0.5 m bins size, but at a slower sampling rate of 2 Hz. All ADCPs were set to measure in bursts of 1024 samples, separated by intervals of 30 minutes. Concurrent with the velocity measurements, and at the same sampling rates, all of the instruments recorded pressure, converted into water depth. All ADCPs were deployed on low profile (trawl proof) moorings.

3.3.2. Turbulence measurements

Turbulence measurements were collected at Criterion Jetty (51°41.98′N, 4°56.68′W) as part of the testing of a scale prototype of a self recovering instrument frame (an acoustically operated, compressed gas solution designed to house a converging beam acoustic Doppler device that was designed and constructed under the EU ERDF Selkie Project). A Nortek Vector acoustic Doppler velocimeter (ADV) was installed on the frame, which was deployed from 19 May – 4 June 2021, covering one spring-neap cycle. The ADV was positioned such that the measurement volume was 1.15 m above the seabed – higher in the water column than any other parts of the frame, and so relatively undisturbed. Three dimensional (3D) velocity data was collected continuously throughout the deployment at 32 Hz. Post-recovery data was de-spiked based on deviation from a 5-minute rolling average and removing any points that had deviations greater than one standard deviation of the entire record. Turbulent kinetic energy (TKE), k, is then calculated from the variances of the velocity components using:

$$k = \frac{1}{2}(\overline{(u')^2} + \overline{(v')^2} + \overline{(w')^2}) \tag{1}$$

Then the turbulent intensity (TI) can be calculated from k and the

Reynolds-averaged mean flow U, using:

$$TI = \frac{\sqrt{\frac{2}{3}k}}{U} \tag{2}$$

3.4. Wave measurements

Wave buoy data was collected at both the Dale Roads wave test site and the East Pickard wave & floating wind site. Data was collected using a Datawell Directional Waverider MkIII, moored in 14 m water depth, at Dale Roads between 2 December 2019 and 14 June 2021 as part of the SEACAMS (ERDF) project. Data was collected at East Pickard using an AXYS Technologies Triaxys directional wave buoy, moored in 27 m water depth, between 27 March 2019 and 4 March 2020 – this data was collected by META to support their activities. There is also wave data farther offshore at the Pembrokeshire Demonstration Zone which can be used to consider scaling parameters of the test sites; this data was collected with a Datawell Directional Waverider MkIII. The site was originally run by the SEACAMS project, but since October 2019 the site has been operated by the Cefas Wavenet[4] programme – a UK wave monitoring network.

The wave buoys return standard wave parameters (significant wave height, mean, peak and energy (for Dale Roads) wave periods and direction), and one-dimensional wave spectra. The wave energy period is typically used for wave energy characterization; this is not reported for the East Pickard site but can be estimated from the mean period, if a JONSWAP spectrum is assumed [11], using:

$$T_e = 1.18 T_z \tag{3}$$

Wave power, or wave energy flux, is an important quantity when considering energy extraction. It needs to be calculated from buoy measurements, using:

$$P = EC_g \tag{4}$$

where E is the wave energy and C_g is the wave group velocity. The wave energy can be calculated from the wave spectra using

$$E = \rho g m_0 \tag{5}$$

where ρ is the seawater density, g is gravity and m_0 is the zeroth spectral moment.

[4] `https://wavenet.cefas.co.uk/`

4. META site characterization

4.1. Bathymetry

4.1.1. Quayside (phase 1) sites

Carr Jetty, Mainstay Quay and Ferryside (Fig. 2) are predominantly inter-tidal sites immediately adjacent to deeper water (dredged) areas with depths to 15 m, located 300 m to the south of the main estuary channel. Quay 1 is an inter-tidal site to the south of the main estuary channel adjacent to a sloping seabed increasing in depth from $9 - 15$ m over a distance of 180 m towards the NW. Criterion Jetty lies adjacent to a deep-water channel feature (depth $25 - 28$ m) within the main estuary.

4.1.2. Open Water (phase 2) sites

Warrior Way (Fig. 2, Fig. 3) is situated in the main estuary channel to the east of the Cleddau Bridge and orientated NW-SE with water depths generally in the range $16 - 18$ m. Maximum water depths of 22 m are located to the southeast, adjacent to the shallowest region (9 m) located to the northeast of the site where the estuary orientation turns SW-NE. Much of the seabed comprising the northern side of the East Pickard Bay (Fig. 4) to the east of the estuary entrance is characterized by the presence of a N-S and E-W sloping, strongly faulted, bedrock shelf extending 350 m south and parallel to the coastline at depths ranging between 8 m and 20 m. The bedrock shelf terminates abruptly giving rise to an adjacent area characterized by an E-W gently sloping seabed surface with depths extending from 12 m at the northern end of Freshwater West to 26 m, 2400 m to the west, approximately 1 km south of Whitedole Bay. The Dale Roads site (Fig. 5) is characterized by a gentle southerly sloping seabed, with depths ranging from $12 - 15$ m over a distance of approximately 600 m. The southwest section of the site is characterized by a 150 m wide, irregular bedrock outcrop extending over 500 m, orientated NW-SE with isolated high points up to 8 m. The seabed surrounding this outcrop appears relatively featureless with no sedimentary bedforms present. Multibeam data from the area further south and west suggests that the vertical extent of seabed sediments throughout this region of the Haven are limited or absent due to the proximity of the underlying bedrock relative to the seabed surface.

4.2. Tidal elevations

From the 70 year elevation dataset recorded at Milford Haven, the maximum continuous record was 14 February 2001 to 27 July 2003 (893 days).

This time series (with a time step of 15 minutes) was harmonically analyzed using *t_tide* [12] and the tidal constituents with amplitude greater than 5 cm are listed in Table 3. Although the Solar annual constituent (SA) was calculated as around 6.4 cm, it was associated with a relatively large error in the harmonic analysis and so is not included in Table 3.

The tides are strongly semi-diurnal, with an M2 (S2) amplitude of 2.203 m (0.801 m) and a Form Factor[5] of 0.044. Spring/mean/neap tidal ranges are around 6.3/4.4/2.7 m. The tidal elevations are also characterized by strong lunisolar (K2) and larger lunar elliptic (N2) semidiurnal constituents, leading to relatively large variations in successive spring/neap cycles. This has implications in the time period used for measurements or technology testing as there will be significant differences in spring tides (for example) every two weeks.

4.3. Mean flow conditions

4.3.1. Depth-averaged currents

At Warrior Way East, the 19 day time series shows peak (depth-averaged) current speeds of around 1 m/s (Fig. 6). There is strong flood/ebb asymmetry in the tidal currents, with a typical spring ebb current of 1 m/s being followed by a typical flood current of 0.8 m/s. Tidal analysis of the currents (Table 4) shows that this asymmetry is due to shallow water constituents (at both fourth and sixth diurnal frequencies) at Warrior Way East, and at the other two ADCP locations. The longer (47 day[6]) deployment at Warrior Way West captured multiple spring-neap cycles (Fig. 7). This site is more energetic than Warrior Way East, with peak spring current speeds up to 1.4 m/s. Again, there is strong asymmetry in the tidal currents. A peak ebb current speed of 1.4 m/s is followed by a peak flood current speed of around 0.8 m/s. By converting the currents into power, this results in large differences in peak power densities of 1400 kW/m^2 (ebb) followed by 262 kW/m^2 (flood) (since the current speed is cubed), i.e. a factor of five. The longer time series also demonstrates that there are large differences in current speeds between successive spring-neap cycles; for example the peak ebb spring current speed is around 1.2 m/s on the 13 April, but exceeds 1.4 m/s on the 28 April. The source of this variation can be attributed to the large N2 current amplitude

[5]Ratio of (K1+O1) to (M2+S2) amplitudes.

[6]Although only 28 days of this time series was usable due to a shift in the mooring

at this location (0.154 m/s), which is approximately 50% of the S2 amplitude (Table 4). Criterion Jetty is much less energetic than the other sites, with peak currents of around 0.6 m/s (Fig. 8). The depth-averaged currents for all three locations are compared as 'tidal ellipses' in Fig. 9, confirming the strong magnitude asymmetry between the flood and ebb phases of the tidal cycle, yet associated with minimal directional asymmetry.

4.3.2. Depth-varying currents

The three ADCP deployments (Table 2) allow the hydrodynamics to be analyzed throughout the water-column (except near surface and near seabed) and quantified through harmonic analysis. Harmonic analysis was performed using least-squares fitting *t_tide* package ([12]) on the north-south (v) and east-west (u) components of depth-averaged current and the current time-series at each "bin" (ensemble-averaged height above the seabed: see Table 2). The time-series figures of observed currents, in depth and time, are shown in Fig. 10, Fig. 11, and Fig. 12, for Warrior Way East, Warrior Way West, and Criterion Jetty, respectively.

The time-series (top panel in Fig. 10, Fig. 11, and Fig. 12) was harmonically analyzed, with "non-harmonic flow", i.e. any residual currents remaining that could not be accounted with harmonics, given an error in both time (summed throughout the water-column) and throughout the water-column (summed through time) calculated. Near-surface bins, where data was missing due to the tidal range introducing gaps in the tidal current time-series, were removed from the analysis – further reducing the amount of data, but necessary due to the increasing error (σ_{RMSE}) near the surface. At all three sites, no correlation to error (or non-harmonic "weather" flows) was found – for example with observed wind speed at the port of Milford Haven ($R^2 < 1\%$). Instead, the non-harmonic flow is likely to be due to unresolved harmonic features within the tide: as can be seen by the regular periodicity in the time-series error of Fig. 10.

Further characterization of the tidal flow was performed at the three ADCP sites by grouping data into "flooding" (tidal currents from Low Water to High Water) and "ebbing" (tidal currents from High Water to Low Water); as described in Lewis et al. [13], assuming a standing wave system. All sites have near-rectilinear flow conditions, and flood-ebb asymmetry is in current magnitude only (Fig. 9). Further analysis, with the curve fitting profile described in Lewis et al. [13], shows that the velocity profiles have minimal shear at these sites, with near plug flow ($\sim$ 1/14th power law) instead of

1/7th power law found in more "open coastal" tidal energy sites as shown in Table 5; where the velocity at a specific height above bed (U_z) can be described using the depth-averaged flow ($\overline{U}$), water depth, and the power (α) and roughness (β) coefficients:

$$U_z = \left(\frac{z}{\beta h}\right)^{1/\alpha} \overline{U} \tag{6}$$

Therefore, we find tidal flows at Warrior Way and Criterion Jetty are heavily modified by friction, with flood-ebb asymmetry in current magnitude and velocity profile shape – suggesting seabed feature generated effects are influencing flow conditions (e.g. Fig. 3). Indeed, Criterion Jetty showed much greater variability and difference between the flood and ebb tides, whilst Warrior Way had a similar pattern on either side and, relatively, lower variability in space and time (see Fig. 13) – hence Warrior Way appears to have favourable conditions for hydrokinetic energy device deployments.

4.4. Turbulence properties

Turbulent Kinetic Energy (TKE) for Criterion Jetty is plotted against mean velocity (Fig. 14), with a clear, if unsurprising, trend of TKE increasing with increasing mean velocity. Turbulence Intensity (TI) is shown in Fig. 15. There is greater variability at lower velocities, and there are higher TI values associated with lower mean velocities due to mean velocity being the denominator in Eq. 2, similar to other studies, e.g. [14]. The mean value for TI is 0.55 or 55%, which is high compared to many tidal stream sites, where values of $5 - 35\%$ have been reported [15, 16, 17]. This may be due to the generally low mean velocities at Criterion Jetty (e.g. peak spring current of 0.6 m/s) compared to grid-connected commercial sites where current speeds are often in excess of 2.5 m/s [18]. On the flood phase of the tidal cycle, there are minimal bed features upstream, and so turbulence is bed-generated. On the ebb phase of the tidal cycle, there is a large meandering channel and bridge pilings 1 km upstream, all of which may generate additional turbulence. Given the shallow water depths at Criterion Jetty, minimal depth variation in turbulence is expected.

4.5. Wave climate

Wave roses were calculated for both wave energy test sites (Fig. 16). Wave heights are greater at the more exposed East Pickard site, and there

is greater variability (compared to Dale Roads) about the predominant wave direction (from the WSW). Refraction into the Milford Haven Estuary means that waves at Dale Roads are predominantly incident from the SSW. Joint $H_s - T_e$ occurrence matrices are shown for Dale Roads (Fig. 17) and East Pickard (Fig. 18). Fig. 19 displays time series of wave power at the two sites. Time periods are not concurrent, but similar seasonality can be seen at both sites with typically higher values in the winter months; however, it should be noted that energetic storms can occur at any time of year. Mean values of key parameters for both sites are summarized in Table 6.

One of the benefits of the META suite of test locations is the proximity to the PDZ (see Section 1). Therefore it is instructive to consider the scaling factors between both Dale Roads & East Pickard and the PDZ. Based on Froude scaling, wave heights scale linearly, and comparison can be used to identify the scale factor between sites. For perfect scaling, wave heights should then scale by the square root of the scale factor. Given the influence of water depth on wave characteristics, site water depth should also scale linearly with the wave height scale factor. In this section, line fitting to scatter plots is used to establish scale factors. Due to data availability, scaling estimates are made for different time periods for both test sites: for Dale Roads, a year of data between 01/02/2020 and 31/01/2021 was used; however for East Pickard, larger data gaps meant comparison was made between 15/06/2019 – 14/10/2019, 22/10/2019 – 06/11/2019, and 23/01/2020 – 03/04/2020.

Fig. 20 shows scatter plots for various parameters at Dale Roads and the PDZ; lines of best fit of the form $y = mx$ are plotted for each parameter. Forcing the intercept to zero allows the gradient to equal the scale factor. This gives a scale factor of 0.31, or approximately 1/3 between Dale Roads and the PDZ. Based on Froude scaling, the scale factor for the wave period should be 0.56; in fact, the gradient is 0.82 for the mean period and 0.95 for peak periods. Energy period is not shown, because measured values are not available for East Pickard or for the PDZ data collected by Cefas. It is unsurprising that peak periods are so similar, given the close proximity of the two buoys and the fact that while energy may be redistributed due to wave transformation processes, peak period is unlikely to be altered. Differences in scale factor between wave height and period is something that has been noted at other real-world scale test sites. Directional spreading is slightly lower at the Dale Roads site, presumably due to its more constrained location. The scale factor between water depths at the two sites is 0.25 (14 m at Dale Roads,

56 m at PDZ). This means that water depths and wave heights have similar scaling and so, despite the less satisfactory wave period scaling, Dale Roads can be considered a scale site for the PDZ with a scale factor of 1/3. When the same plot is created for the comparison between East Pickard and the PDZ, it can be seen that the wave climate at both sites is very similar. While East Pickard is further inshore and in shallower water, it is just as exposed to the predominant SW and W wave incidence as the PDZ. Therefore the scaling of waves is 0.8, and both mean and peak period scaling is > 0.95. This means East Pickard is not a useful scale site for the PDZ, but should be considered as a scale site for more energetic areas or as a useful location for nearshore full scale testing prior to deployment at the PDZ.

5. Discussion

The META data

The primary tidal test site (Warrior Way) has water depths in the range $10 - 20$ m, suitable for testing TRL 4–6. However, it should be noted that a spring tidal range of 6.3 m could present a challenge for some devices (e.g. at the shallower end of Warrior Way total water depth will vary between $7-13$ m during a spring tide), and could favour testing of floating technologies. This is in contrast to EMEC, where the tidal range is around 2.3 m (spring) [19]. The sea bed at the more exposed wave test sites is generally characterized as bed rock, much in agreement with any other high energy wave energy test or commercial sites (e.g. [20]). All investigated sites within the Milford Haven waterway were strongly asymmetrical due to shallow water harmonics at fourth and sixth diurnal frequencies. Since power is proportional to velocity cubed, this asymmetry is amplified in power output, but the Fall of Warness in Orkney is also an example of an asymmetrical test site [21], yet has been a successful test location over the last 15 years. This would not be the case at a commercial site, where asymmetry in power output would be undesirable. Examination of how the current speed varies over the water column shows minimal shear at these sites, with near plug flow ($\sim$ 1/14th power law) instead of the classical 1/7th power law commonly found at other tidal energy test locations (e.g. [22]). Turbulence intensities are higher at the Criterion Way site (55%) than is often reported in the literature for prospective tidal stream energy sites, which are typically $5-35\%$ [15, 16, 17]. This finding will be important for developers to consider when conducting early stage tests at

this location, because turbulence induced stresses would be proportionally greater than at full-scale.

The wave climate and water depths at the Dale Road site provide a good 1/3 scale test site for the neighbouring Pembrokeshire Demonstration Zone (PDZ). Conditions at the East Pickard location are similar to the PDZ, with a wave height scale factor of 4/5. Therefore, this site is better considered as a scale site for more energetic locations. Given that East Pickard is *en route* from Milford Haven to the PDZ, it may prove a useful site for short-term full-scale testing prior to deployment of devices at the PDZ.

Additional data collection

The data collected from META is already extensive, particularly the multibeam data coverage, but further data would be useful in characterizing the site both spatially and temporally.

Further multibeam surveys would provide complete coverage across the sites, and such data would also assist in parameterizing model bathymetry (see next sub-section). Also, many regions of the Milford Haven waterway are dredged, and up-to-date multibeam surveys would help characterize changes in the sea bed over time.

The three ADCP moorings presented here offer a robust initial overview of tidal dynamics across META, but further deployments at multiple locations, and covering different time periods will further refine the site characterization. It has been noted that nodal corrections over an 18.6 year cycle can lead to an error exceeding $\pm 10\%$ in annual energy yield (AEY) depending on the year selected for data collection [23], and so repeat surveys, even at the same locations, can be useful in further quantifying and characterizing the tidal energy resource, including resolving additional tidal constituents than those presented here (Table 4). In addition to point sensors, further spatial surveys in the region to characterize the currents could include ADCP transects [24] and novel methods of data collection such as drone-based large-scale particle image velocimetry [25] and X-band radar [8]. Further information about turbulent properties at the other tidal test locations in the META suite of facilities (i.e. beyond the low energy Criterion Jetty site) would be beneficial to developers. A converging beam ADCP array (comprised of three ADCPs), specifically built for improved turbulence measurements at tidal energy sites, has recently been deployed at the Warrior Way site as part of the Selkie Project, and tests are underway.

Numerical model development

The evidence presented in this paper is based entirely on *in situ* data. Although wave properties, and to a lesser extent tidal properties, will change over longer timescales[7], it is also useful to use numerical models to simulate the waves and tides of the region, e.g. to investigate scenarios that have not necessarily been captured by the observations (e.g. extreme events), and also to provide consistent spatial and temporal coverage of the region. Such a model (or series of models) could be parameterized and calibrated/validated by the data presented in this study. Since models are often validated outside of the region of interest, providing confidence in the wave/tidal properties throughout the computational domain, they can be used to investigate near-field and far-field environmental impacts, including feedbacks between devices and the resource.

Future of META

At the time of writing, META has been fully operational for 1 year and has started to develop a project pipeline. The types of experimental devices that are planned to test at META in the near-to-medium future include tidal turbines, wave energy convertors, offshore hydrogen systems, and various novel sub-assemblies, components, and scientific instruments. Since the META initiative was conceived in 2017, the offshore renewables industry has evolved, with increased interest in testing floating offshore wind, hydrogen, floating solar, hybrid and co-located systems, and automated and robotic systems. In turn, the META facility will primarily continue to support wave and tidal technology testing, but where possible expand its offering to accommodate these other marine technologies which have a role in the renewable energy transition. This may involve varying consents at existing sites, or developing new sites in and around the Milford Haven Waterway.

Some important objectives for META to ensure future success are to continue adding value to the facility in terms of data, infrastructure, and equipment availability; an ability to adapt to meet diverse marine technology requirements; and to pursue collaboration with existing and new partners to create a hub for research, development and innovation around the META facility.

[7] E.g. due to sea-level rise/climate change or inter-annual variability.

6. Conclusion

This article has presented analysis and synthesis of the various datasets that have been collected from the META sites over the past decade. The results demonstrate the opportunities and challenges associated with testing at META, e.g. strong asymmetry in the tides. We have highlighted gaps in data from both spatial and temporal perspectives, and how future data collection, and the development of a numerical model of the region, will support wave and tidal technology testing, in addition to providing the flexibility to expand into testing other marine energy technologies such as floating wind and solar, and co-located devices.

Acknowledgements

The Bangor University researchers acknowledge the support of the Smart Efficient Energy Centre (SEEC), and SEACAMS I, II, all projects funded by the Welsh European Funding Office (WEFO) as part of the European Regional Development Fund (ERDF). The researchers at Swansea University also acknowledge the support of SEACAMS I, II, in addition to Selkie, a project that was funded by the ERDF through the Ireland-Wales Cooperation programme.

Data availability

The multibeam and ADCP data are available from the IMARDIS data portal https://portal.imardis.org/. The wave data for Dales Roads is available from Cefas WaveNet https://www.cefas.co.uk/data-and-publications/wavenet/, and the East Pickard wave data is available upon reasonable request from Marine Energy Wales. The tide gauge data are available from the British Oceanographic Data Centre (BODC) https://www.bodc.ac.uk/data/hosted_data_systems/sea_level/uk_tide_gauge_network/

References

[1] V. Marti, J. Culina, S. Neill, Ocean renewable energy test centers, in: Comprehensive Renewable Energy, 2022.

[2] B. Gaurier, G. Germain, J.-V. Facq, C. Johnstone, A. Grant, A. Day, E. Nixon, F. Di Felice, M. Costanzo, Tidal energy "Round Robin" tests comparisons between towing tank and circulating tank results, International Journal of Marine Energy 12 (2015) 87–109.

[3] R. Yemm, D. Pizer, C. Retzler, R. Henderson, Pelamis: experience from concept to connection, Philosophical Transactions of the Royal Society A: Mathematical, Physical and Engineering Sciences 370 (1959) (2012) 365–380.

[4] M. Lewis, R. O. Murray, S. Fredriksson, J. Maskell, A. de Fockert, S. P. Neill, P. E. Robins, A standardised tidal-stream power curve, optimised for the global resource, Renewable Energy 170 (2021) 1308–1323.

[5] M. Piano, S. Ward, P. Robins, S. Neill, M. Lewis, A. Davies, B. Powell, A. W. Owen, R. Hashemi, Characterizing the tidal energy resource of the west Anglesey Demonstration Zone (UK), using Telemac-2D and field observations, in: Proceedings of the XXII TELEMAC-MASCARET Technical User Conference October 15-16, 2042, 2015, pp. 195–203.

[6] R. Roche, K. Walker-Springett, P. Robins, J. Jones, G. Veneruso, T. Whitton, M. Piano, S. Ward, C. Duce, J. Waggitt, et al., Research priorities for assessing potential impacts of emerging marine renewable energy technologies: Insights from developments in Wales (UK), Renewable Energy 99 (2016) 1327–1341.

[7] S. P. Neill, M. J. Lewis, M. R. Hashemi, E. Slater, J. Lawrence, S. A. Spall, Inter-annual and inter-seasonal variability of the Orkney wave power resource, Applied Energy 132 (2014) 339–348.

[8] S. P. Neill, K. A. Haas, J. Thiébot, Z. Yang, A review of tidal energy–resource, feedbacks, and environmental interactions, Journal of Renewable and Sustainable Energy 13 (6) (2021) 062702.

[9] A. Sentchev, M. Thiébaut, F. G. Schmitt, Impact of turbulence on power production by a free-stream tidal turbine in real sea conditions, Renewable Energy 147 (2020) 1932–1940.

[10] T. Blackmore, L. E. Myers, A. S. Bahaj, Effects of turbulence on tidal turbines: Implications to performance, blade loads, and condition monitoring, International Journal of Marine Energy 14 (2016) 1–26.

[11] B. Cahill, T. Lewis, Wave period ratios and the calculation of wave power, in: METS2014, 2014.

[12] R. Pawlowicz, B. Beardsley, S. Lentz, Classical tidal harmonic analysis including error estimates in MATLAB using T_TIDE, Computers & Geosciences 28 (8) (2002) 929–937.

[13] M. Lewis, S. Neill, P. Robins, M. R. Hashemi, S. Ward, Characteristics of the velocity profile at tidal-stream energy sites, Renewable Energy 114 (2017) 258–272.

[14] N. S. Lucas, M. J. Austin, T. P. Rippeth, B. Powell, P. Wakonigg, Turbulence and coherent structure characterisation in a tidally energetic channel, Renewable Energy 194 (2022) 259–272.

[15] P. Garcia Novo, Y. Kyozuka, Analysis of turbulence and extreme current velocity values in a tidal channel, Journal of Marine Science and Technology 24 (3) (2019) 659–672.

[16] I. A. Milne, R. N. Sharma, R. G. Flay, S. Bickerton, Characteristics of the turbulence in the flow at a tidal stream power site, Philosophical Transactions of the Royal Society A: Mathematical, Physical and Engineering Sciences 371 (1985) (2013) 20120196.

[17] M. Togneri, I. Masters, Micrositing variability and mean flow scaling for marine turbulence in Ramsey Sound, Journal of Ocean Engineering and Marine Energy 2 (1) (2016) 35–46.

[18] D. Coles, A. Angeloudis, D. Greaves, G. Hastie, M. Lewis, L. Mackie, J. McNaughton, J. Miles, S. Neill, M. Piggott, et al., A review of the UK and British Channel Islands practical tidal stream energy resource, Proceedings of the Royal Society A 477 (2255) (2021) 20210469.

[19] S. P. Neill, A. Vögler, A. J. Goward-Brown, S. Baston, M. J. Lewis, P. A. Gillibrand, S. Waldman, D. K. Woolf, The wave and tidal resource of Scotland, Renewable Energy 114 (2017) 3–17.

[20] EMEC, Billia Croo test site: Environmental statement (2019).

[21] S. P. Neill, M. R. Hashemi, M. J. Lewis, The role of tidal asymmetry in characterizing the tidal energy resource of Orkney, Renewable Energy 68 (2014) 337–350.

[22] M. Thiébaut, A. Sentchev, Asymmetry of tidal currents off the W. Brittany coast and assessment of tidal energy resource around the Ushant Island, Renewable Energy 105 (2017) 735–747.

[23] K. Haas, T. Xu, B. Gunawan, Evaluating measurement based tidal energy resource assessment methods, 2022 Ocean Sciences Meeting (2022).

[24] S. Neill, A. Elliott, In situ measurements of spring–neap variations to unsteady island wake development in the Firth of Forth, Scotland, Estuarine, Coastal and Shelf Science 60 (2) (2004) 229–239.

[25] I. Fairley, B. J. Williamson, J. McIlvenny, N. King, I. Masters, M. Lewis, S. Neill, D. Glasby, D. Coles, B. Powell, et al., Drone-based large-scale particle image velocimetry applied to tidal stream energy resource assessment, Renewable Energy 196 (2022) 839–855.

[26] R. Soulsby, Dynamics of Marine Sands (1997).

Figure Captions

Fig. 1 META test areas in the Milford Haven Waterway and surrounding waters. Quayside (phase 1) sites in orange, open water (phase 2) sites in green. Red lines in (a) are electricity transmission lines. Data from the Ordnance Survey and META.

Fig. 2 Multibeam echosounder bathmetry of Pembroke Dock and Warrior Way. Water depths (in metres) relative to mean sea level. Symbols represent the locations of the ADCP moorings – Criterion Jetty (black square), Warrior Way West (black triangle), and Warrior Way East (black circle). White outlines show the test areas.

Fig. 3 Multibeam echosounder bathymetry of Warrior Way (tidal test site – shown as a white outline). Water depths (in metres) relative to mean sea level. Symbols represent the locations of the ADCP moorings – Warrior Way West (black triangle) and Warrior Way East (black circle). White outlines show the test areas.

Fig. 4 Multibeam echosounder bathymetry of East Pickard Bay (wave & floating wind test site – shown as a white outline). Water depths (in metres) relative to mean sea level.

Fig. 5 Multibeam echosounder bathymetry of Dale Roads (wave test site – shown as a white box). Water depths in metres relative to mean sea level.

Fig. 6 Time series of water surface elevations and depth-averaged current speed at Warrior Way East, 22 April – 10 May 2021.

Fig. 7 Time series of water surface elevations, depth-averaged current speed, and power density at Warrior Way West, 31 March – 29 April 2021. Note that the Warrior Way West mooring shifted during the deployment, and so only 28 days of data (out of the full 47 day record) were used for analysis.

Fig. 8 Time series of depth-averaged current speed at Criterion Jetty, 23 March – 10 May 2021. Difference in successive spring currents (at fortnightly intervals) is mainly due to the N2 tidal constituent, which has a magnitude of 20% and 50% of the M2 and S2 constituents, respectively (Table 4).

Fig. 9 Depth-averaged current ellipses.

Fig. 10 ADCP data time-series at Warrior Way East with surface-affected data removed. (a) is observed current magnitude (m/s), and (b) is the non-harmonic flow (as a percentage of (a)), where the predicted tidal currents (from harmonic analysis) are subtracted from the observed currents. The residual "error" is shown in (c), summed throughout the water-column,

and (d) is the wind speed at Milford Haven. (e) is the time-averaged "error" through the water-column, and (f) shows the relationship between wind speed and residual error summed through the water column.

Fig. 11 ADCP data time-series at Warrior Way West with surface-affected data removed. (a) is observed current magnitude (m/s), and (b) is the non-harmonic flow (as a percentage of (a)), where the predicted tidal currents (from harmonic analysis) are subtracted from the observed currents. The residual "error" is shown in (c), summed throughout the water-column, and (d) is the wind speed at Milford Haven. (e) is the time-averaged "error" through the water-column, and (f) shows the relationship between wind speed and residual error summed through the water column.

Fig. 12 ADCP data time-series at Criterion Jetty with surface-affected data removed. (a) is observed current magnitude (m/s), and (b) is the non-harmonic flow (as a percentage of (a)), where the predicted tidal currents (from harmonic analysis) are subtracted from the observed currents. The residual "error" is shown in (c), summed throughout the water-column, and (d) is the wind speed at Milford Haven. (e) is the time-averaged "error" through the water-column, and (f) shows the relationship between wind speed and residual error summed through the water column.

Fig. 13 Velocity profile fits at each of the ADCP locations: (a) Warrior way East, (b) Warrior Way West, and (c) Criterion Jetty. The light grey lines show the instantaneous fits, and the dark solid lines are the averaged fits for flood (red) and ebb (blue). Dashed lines are one standard deviation either side of this mean. Where there was little variability in the shape and magnitude of the velocity profile, the standard deviation associated with the mean is close together. Sites with little vertical shear in velocity, with little variation in the flow speed at depth or near the surface, have a straighter vertical line.

Fig. 14 The relationship between mean current speed and Turbulent Kinetic Energy at Criterion Jetty (51°41.98′N 04°56.68′W).

Fig. 15 The relationship between mean current speed and Turbulence Intensity at Criterion Jetty.

Fig. 16 Wave roses for East Pickard (left) and Dale Roads (right) based on one year of data at each location (from 03/2019 for East Pickard and 12/2019 for Dale Roads).

Fig. 17 A significant wave height – energy period joint occurrence matrix for one year (2020) of wave data at Dale Roads.

Fig. 18 A significant wave height – energy period joint occurrence matrix

for the East Pickard dataset.

Fig. 19 Time series of wave power for: (a) Dale Roads, and (b) East Pickard.

Fig. 20 Scatter plots of wave parameters for Dale Roads (DR) and the Pembrokeshire demonstration zone (PDZ). Scatter is shaded such that yellows indicate denser regions in the scatter plots. Lines of best fit, of the form $y = mx$, are given as black dashed lines, the gradient of these indicate the scale factor

Tables (including captions)

Category	Site name
Quayside (phase 1) sites	Carr Jetty
	Mainstay Quay
	Ferryside
	Quay 1
	Criterion Jetty
Open water (phase 2) sites	Warrior way (tidal)
	Dale Roads (wave)
	East Pickard Bay (wave & floating wind)

Table 1: List of the META Quayside and Open Water test areas.

	Warrior Way East	Warrior Way West	Criterion Jetty
Deployment latitude	51°42.21′N	51°42.10′N	51°41.99′N
Deployment longitude	04°55.63′W	04°55.31′W	04°56.65′W
Recovery latitude	51°42.20′N	51°42.10′N	51°42.00′N
Recovery longitude	04°55.58′W	04°55.26′W	04°56.60′W
Start date	22 April 2021	23 March 2021	23 March 2021
End date	10 May 2021	10 May 2021	10 May 2021
Water depth (m, relative to MSL)	15.1	19.7	20.1
Instrument	Nortek Signature 500	Nortek Signature 500	RDI Sentinel V
Number of beams	5	5	5
Acoustic Frequency (kHz)	500	500	614
Blanking distance (m)	0.5	0.5	1.68
Bin size (m)	1	1	0.5
Number of bins	28	28	58
Sampling frequency (Hz)	4	4	2
Number of samples per burst	1024	1024	1024
Profile interval (s)	600	600	600
Time between bursts (s)	1800	1800	1800

Table 2: Details of the three ADCP moorings and configurations.

Constituent	Name	Period (h)	H (m)	G (deg)
M4	SW overtide of principal lunar constituent	6.21	0.064	306.2
K2	Lunisolar semidiurnal	11.97	0.231	214.7
S2	Principal solar semidiurnal	12.00	0.801	216.8
L2	Smaller lunar elliptic semidiurnal	12.19	0.120	166.4
M2	Principal lunar semidiurnal	12.42	2.203	172.6
NU2	Larger lunar evectional	12.63	0.086	145.4
N2	Larger lunar elliptic semidiurnal	12.66	0.427	152.6
MU2	Variational constituent	12.87	0.077	188.7
2N2	Lunar elliptic semi diurnal second-order	12.91	0.055	135.4
K1	Lunisolar diurnal	23.93	0.066	130.7
O1	Lunar diurnal	25.82	0.066	354.7

Table 3: Tidal constituents (listed in ascending order of their period) with an amplitude greater than 5 cm based on tidal analysis of 893 days of continuous tide gauge data from Milford Haven. H is amplitude (in metres) and G is phase (in degrees relative to Greenwich). SW = Shallow Water.

Constituent	Name	Warrior Way E.	Warrior Way W.	Criterion Jetty
M2	Principal lunar semidiurnal	0.545	0.656	0.252
S2	Principal solar semidiurnal	0.184	0.304	0.111
N2	Larger lunar elliptic semidiurnal	NA	0.154	0.052
M4	Fourth diurnal shallow water const.	0.061	0.087	0.030
MS4	Fourth diurnal shallow water const.	0.040	0.078	0.029
MSF	Lunisolar synodic fortnightly const.	0.009	0.072	0.025
2MS6	Sixth diurnal shallow water const.	0.054	0.054	0.038
M6	Sixth diurnal shallow water const.	0.065	0.038	0.029
2MN6	Sixth diurnal shallow water const.	NA	0.027	0.021

Table 4: Semi major axis (m/s) for dominant depth-averaged tidal constituents, noting that tidal currents are strongly rectilinear at all three sites (Fig. 9). NA = time period of deployment (19 days) too short to resolve this constituent, i.e. to separate it from constituents that are very close in frequency.

Site	β	flood		ebb	
		α	error (%)	α	error (%)
Warrior Way East	0.4	10	15	13	14
Warrior Way West	0.4	14	17	14	5
Criterion Jetty	0.4	15	5	15	5

Table 5: The velocity profile fitting results for ADCP data at the three sites, using a power law relationship (α) of the Soulsby velocity profile fit [26], as described in Lewis et al. [13]. A lower α value denotes a greater amount of vertical shear in the water column.

Site	H_s (m)	T_p (s)	T_e (s)	T_z (s)	Power (kW/m)	Dir. (°)	Dir. Spr. (°)
Dale Roads	0.57	8.90	6.72	4.55	2.19	196	24.2
East Pickard	1.57	8.88	6.47	5.49	9.42	243	33.40

Table 6: Mean values for significant wave height (H_s), peak period (T_p), energy period (T_e), zero up-crossing period (T_z), wave power (kW/m), peak wave direction and directional spreading.

Declaration of Interest Statement

Declaration of interests

☒ The authors declare that they have no known competing financial interests or personal relationships that could have appeared to influence the work reported in this paper.

☐The authors declare the following financial interests/personal relationships which may be considered as potential competing interests:

CRediT author statement

Simon P. Neill: Conceptualization, Methodology, Formal analysis, Writing - Original Draft, Visualization, Funding acquisition **Iain A. Fairley:** Methodology, Formal analysis, Investigation, Writing - Original Draft, Visualization **Steve Rowlands:** Formal analysis, Visualization **Saul Young:** Writing - Review & Editing **Tom Hill:** Writing - Review & Editing **Christopher A. Unsworth:** Investigation, Writing - Review & Editing **Nicholas King:** Formal analysis, Investigation, Visualization **Michael J. Roberts:** Investigation, Writing - Review & Editing **Martin J. Austin:** Writing - Review & Editing **Peter Hughes:** Investigation **Ian Masters:** Writing - Review & Editing, Funding acquisition **Aled Owen:** Investigation **Ben Powell:** Investigation **Dominic Reeve:** Funding acquisition **Matthew J. Lewis:** Formal analysis, Writing – Original Draft, Visualization

Fig 1

Click here to access/download;Figure;Fig01.jpg

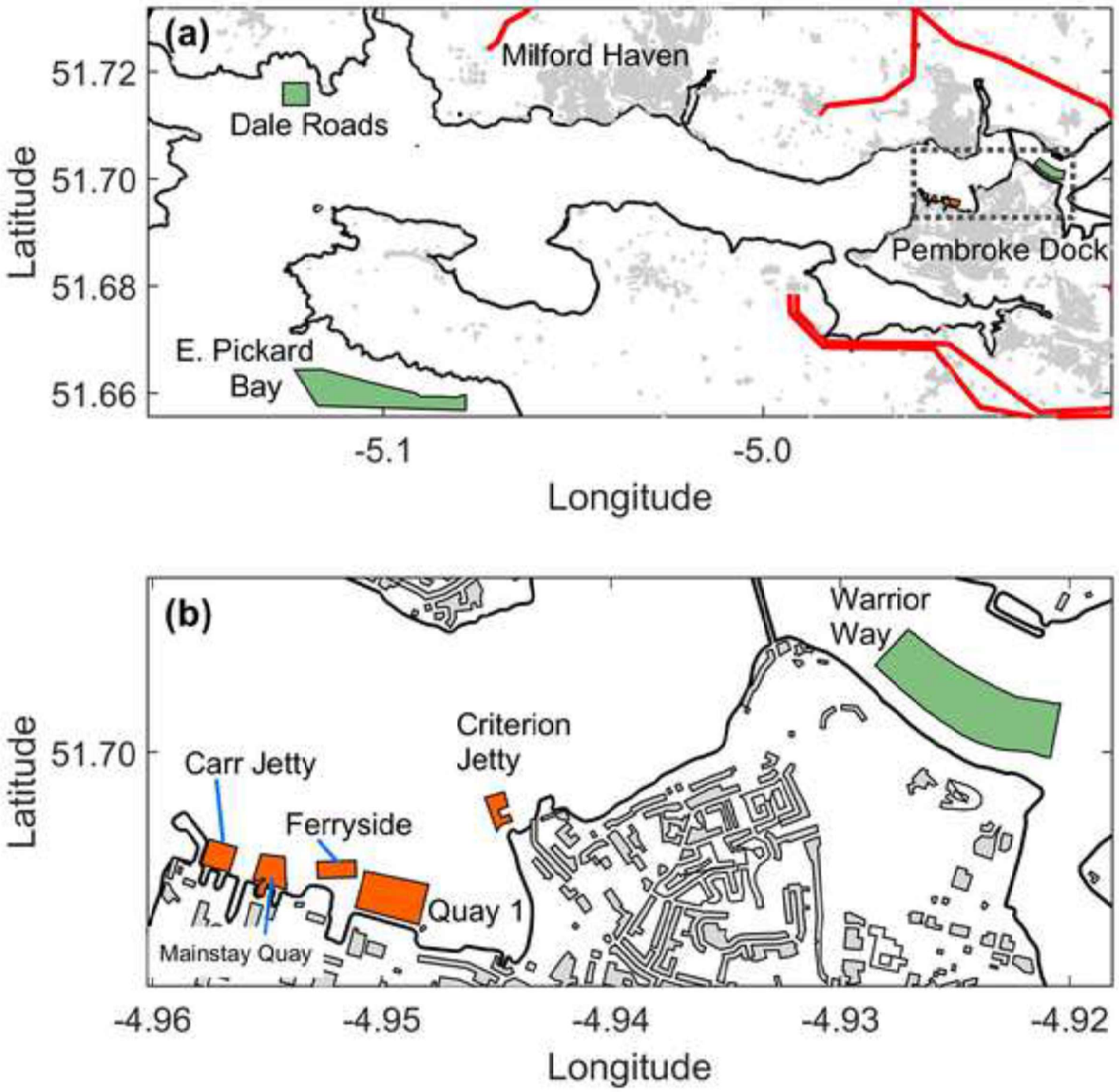

Fig 2

Click here to access/download;Figure;Fig02.jpg

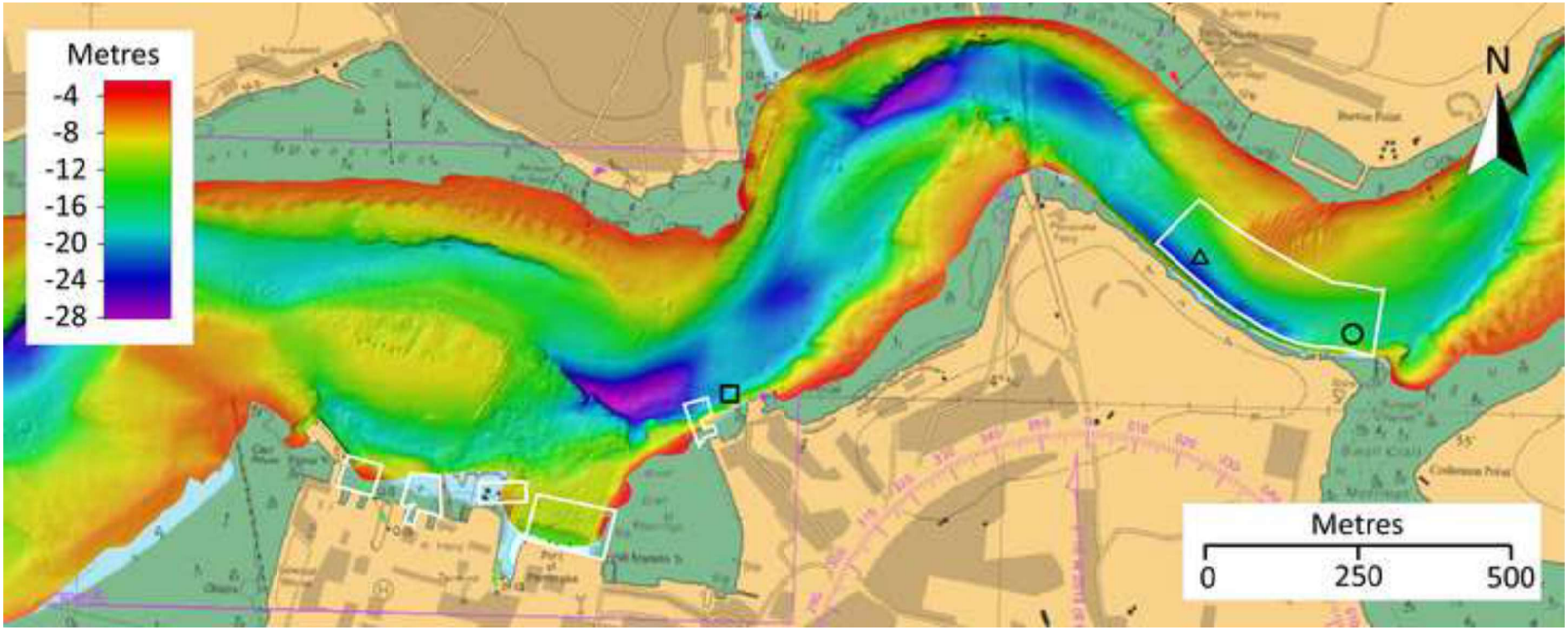

Fig 3

Click here to access/download;Figure;Fig03.jpg

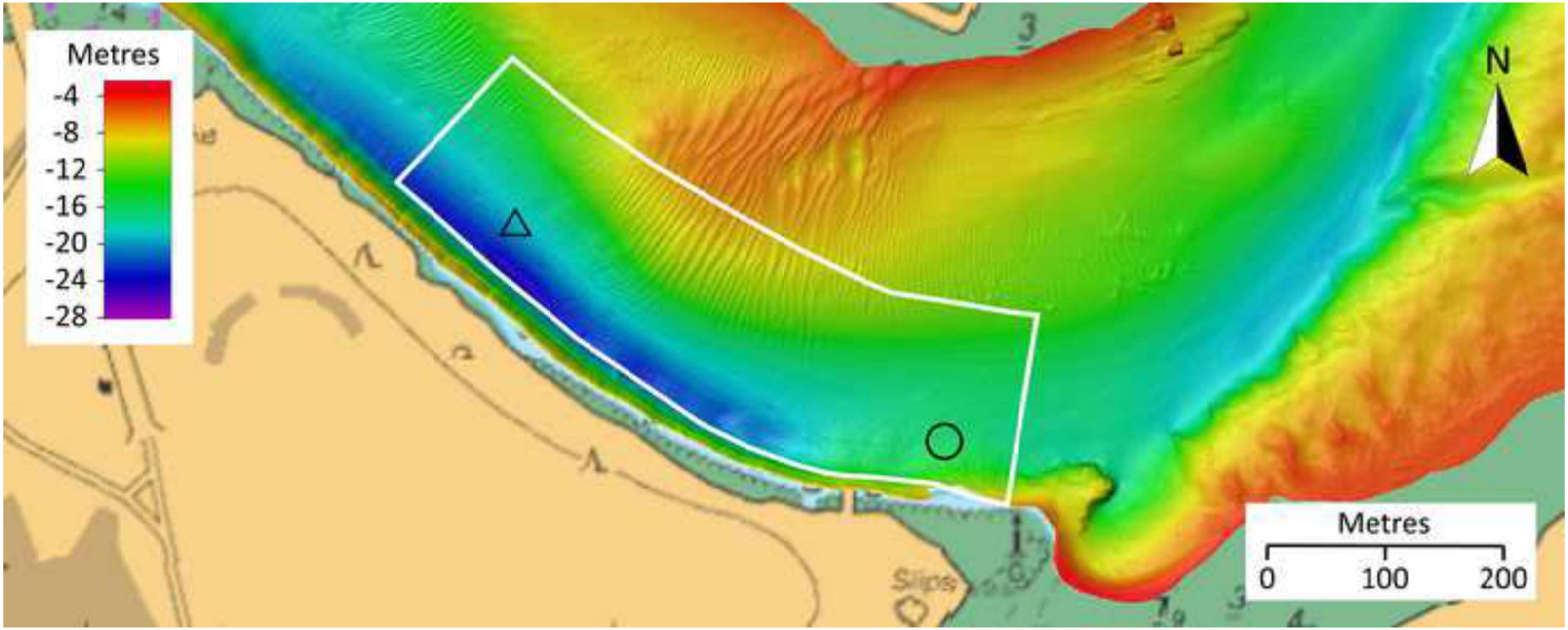

Fig 4

Click here to access/download;Figure;Fig04.jpg

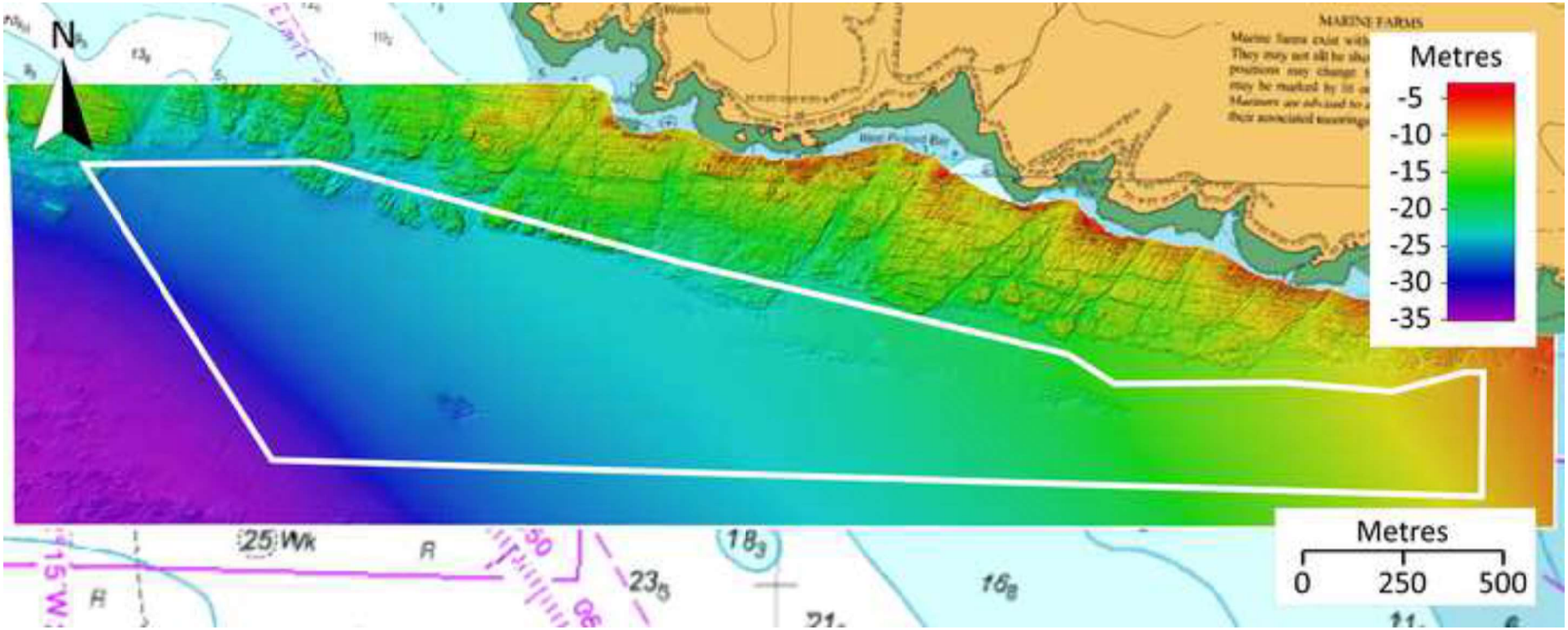

Fig 5

Click here to access/download;Figure;Fig05.jpg

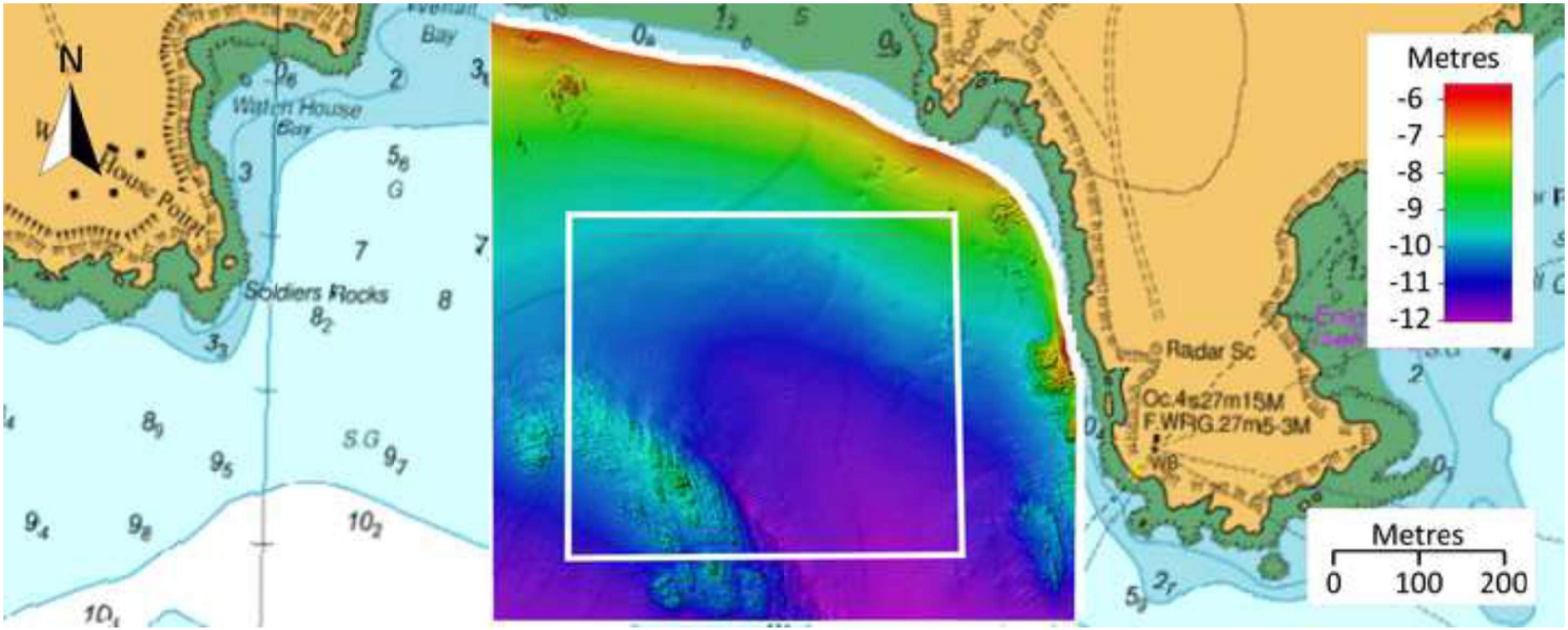

Fig 6

Click here to access/download;Figure;Fig06.png

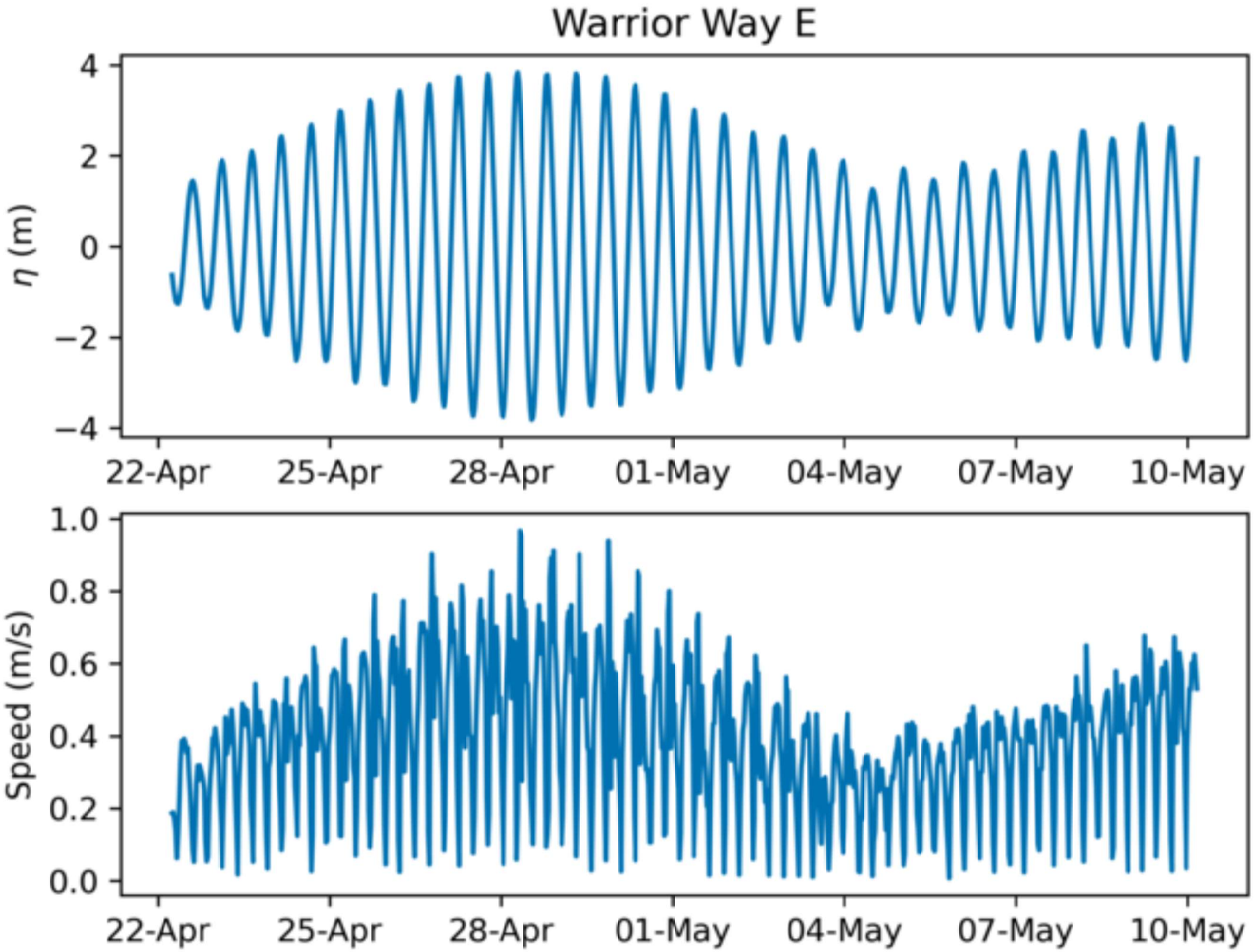

Fig 7

Click here to access/download;Figure;Fig07.png

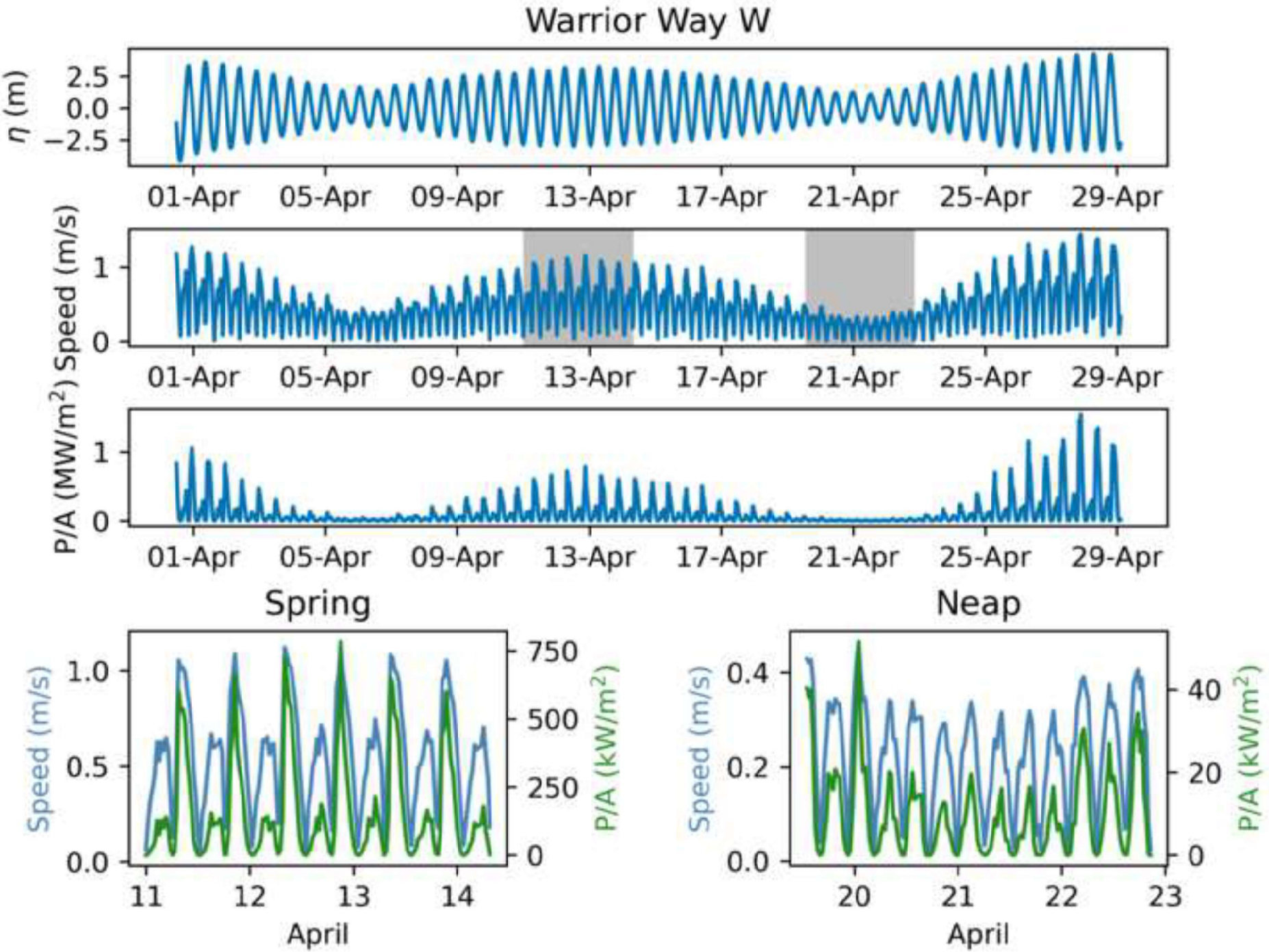

Fig 8

Click here to access/download;Figure;Fig08.png

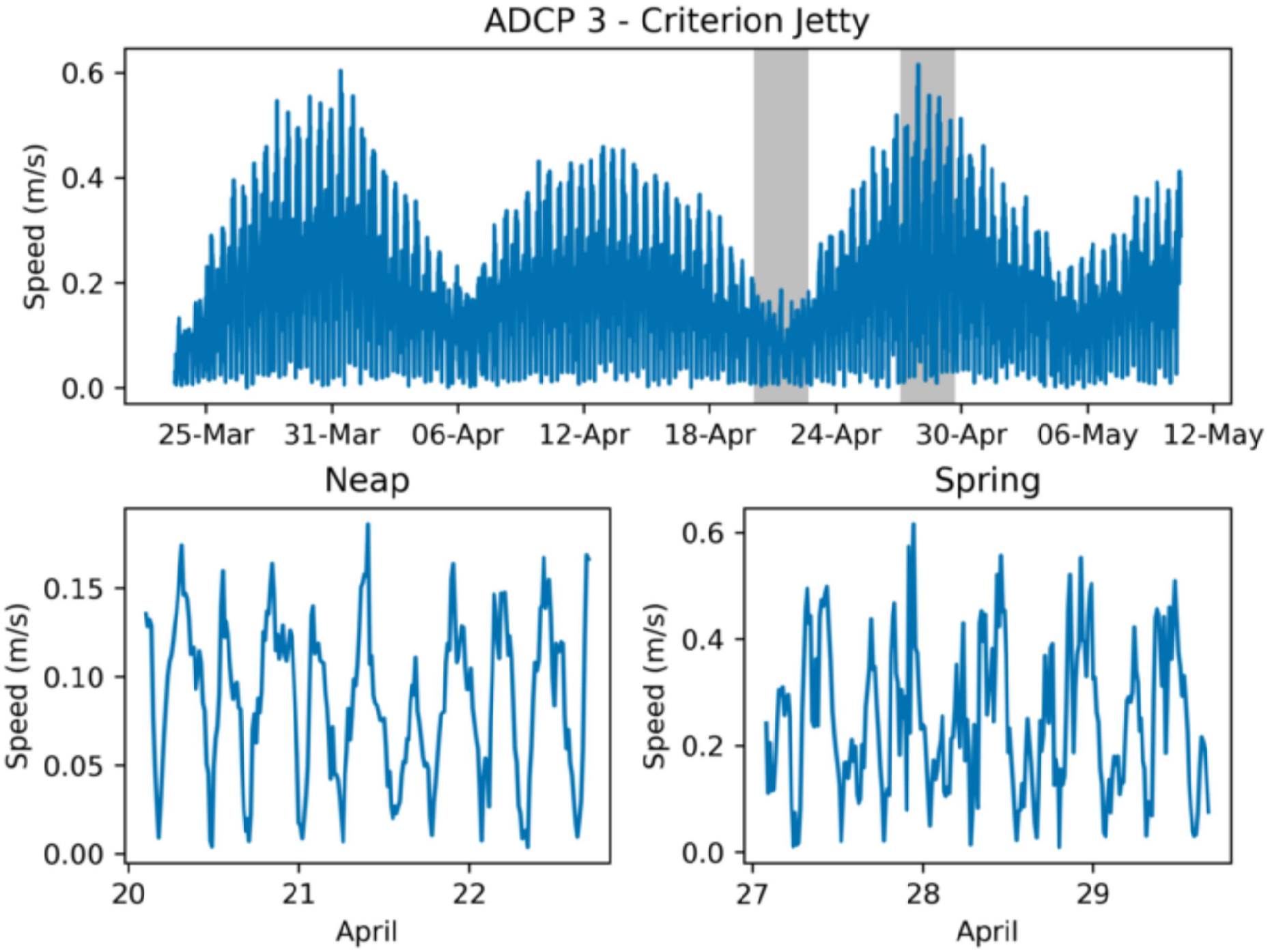

Fig 9

Click here to access/download;Figure;Fig09.png

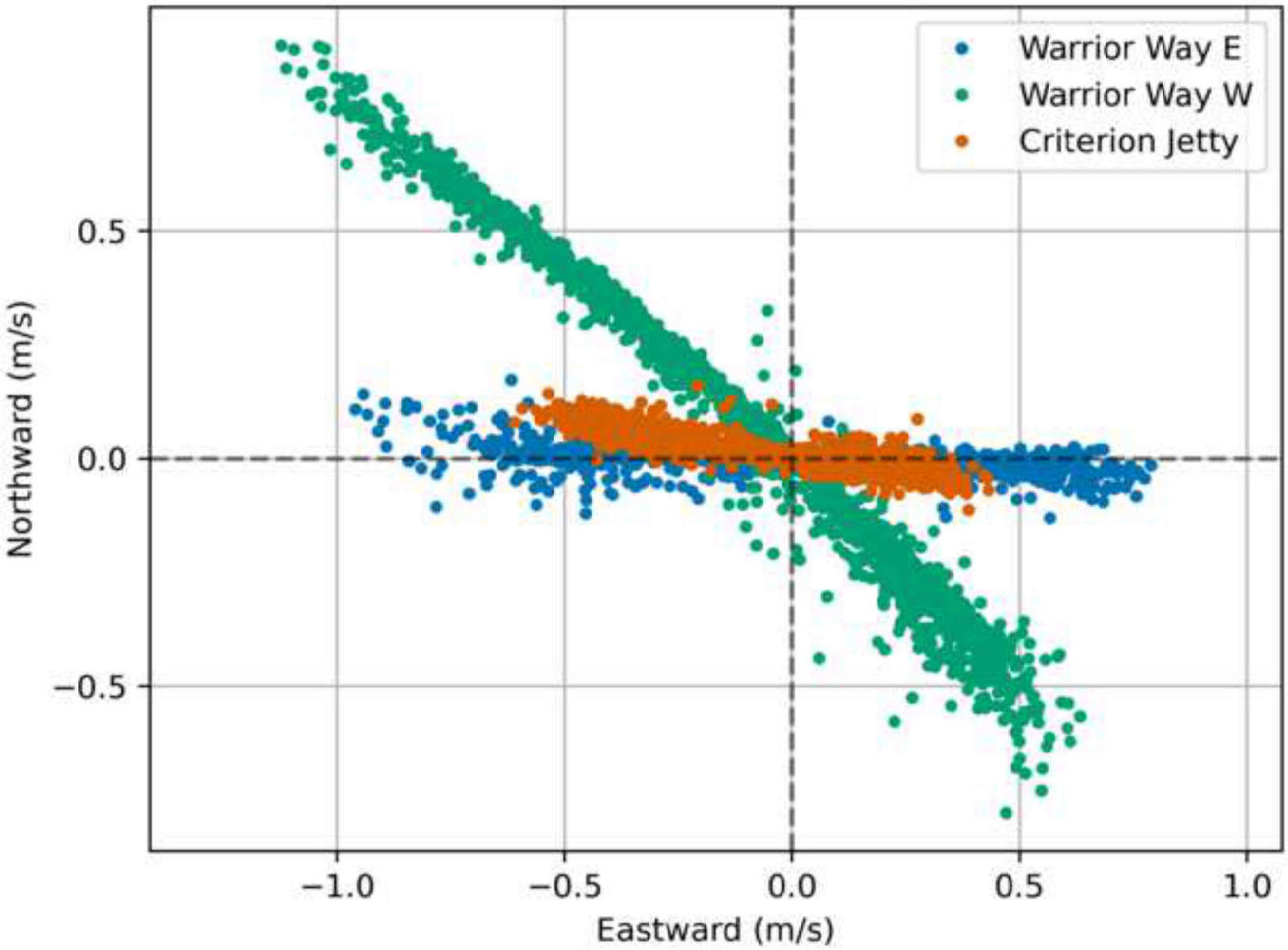

Fig 10

Click here to access/download;Figure;Fig10.jpg

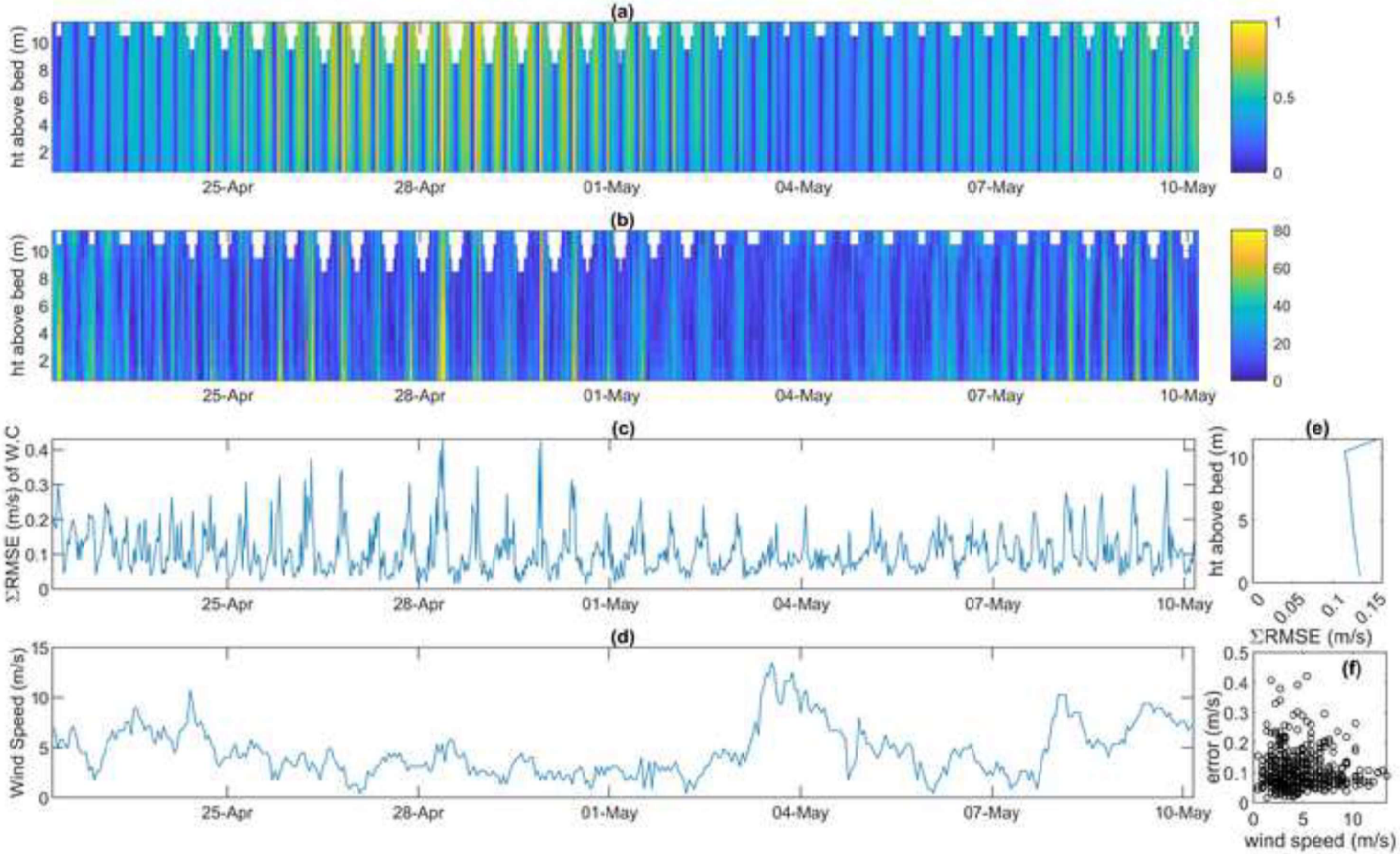

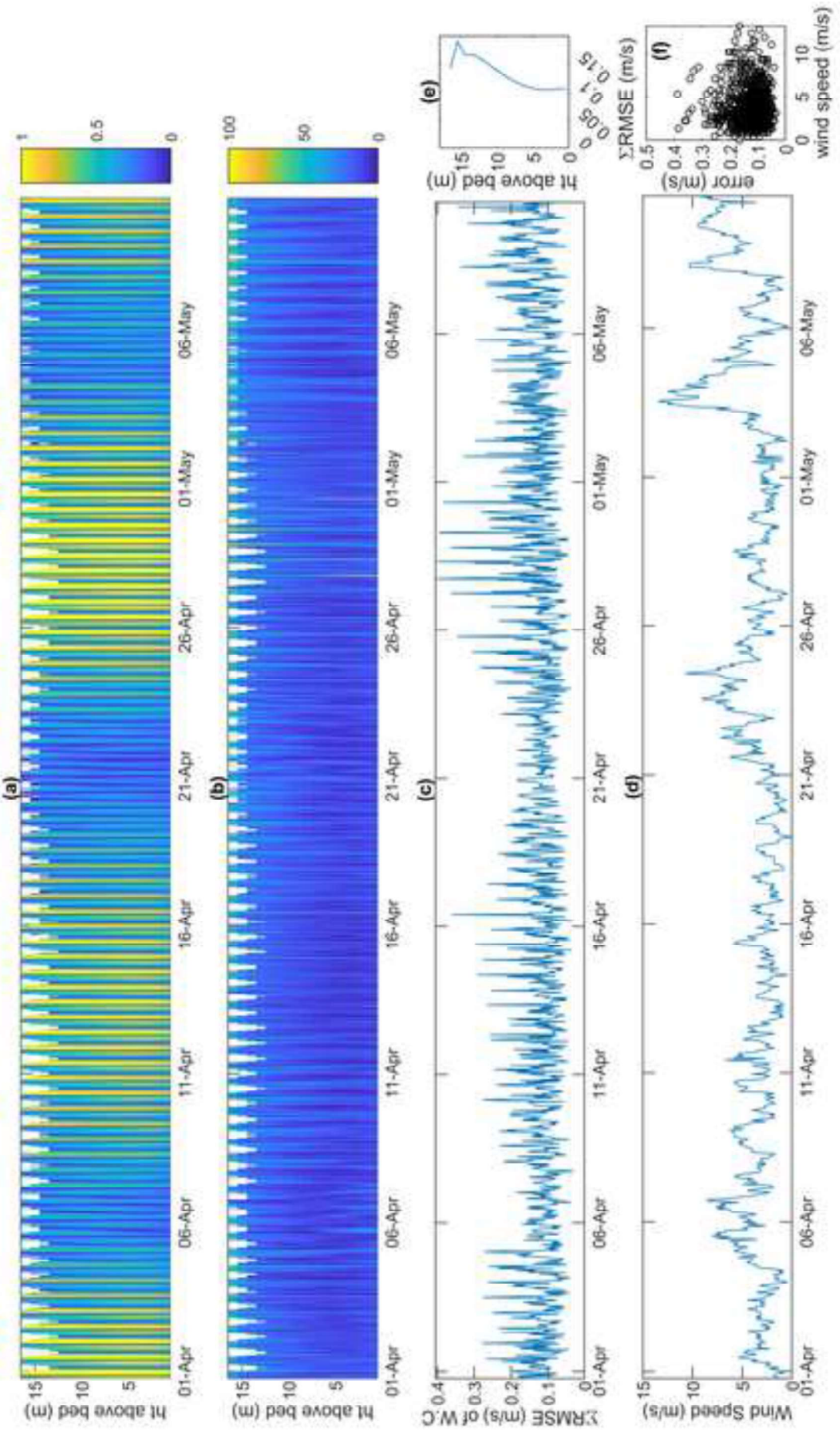

Fig 11

Fig 12

Click here to access/download;Figure;Fig12.jpg

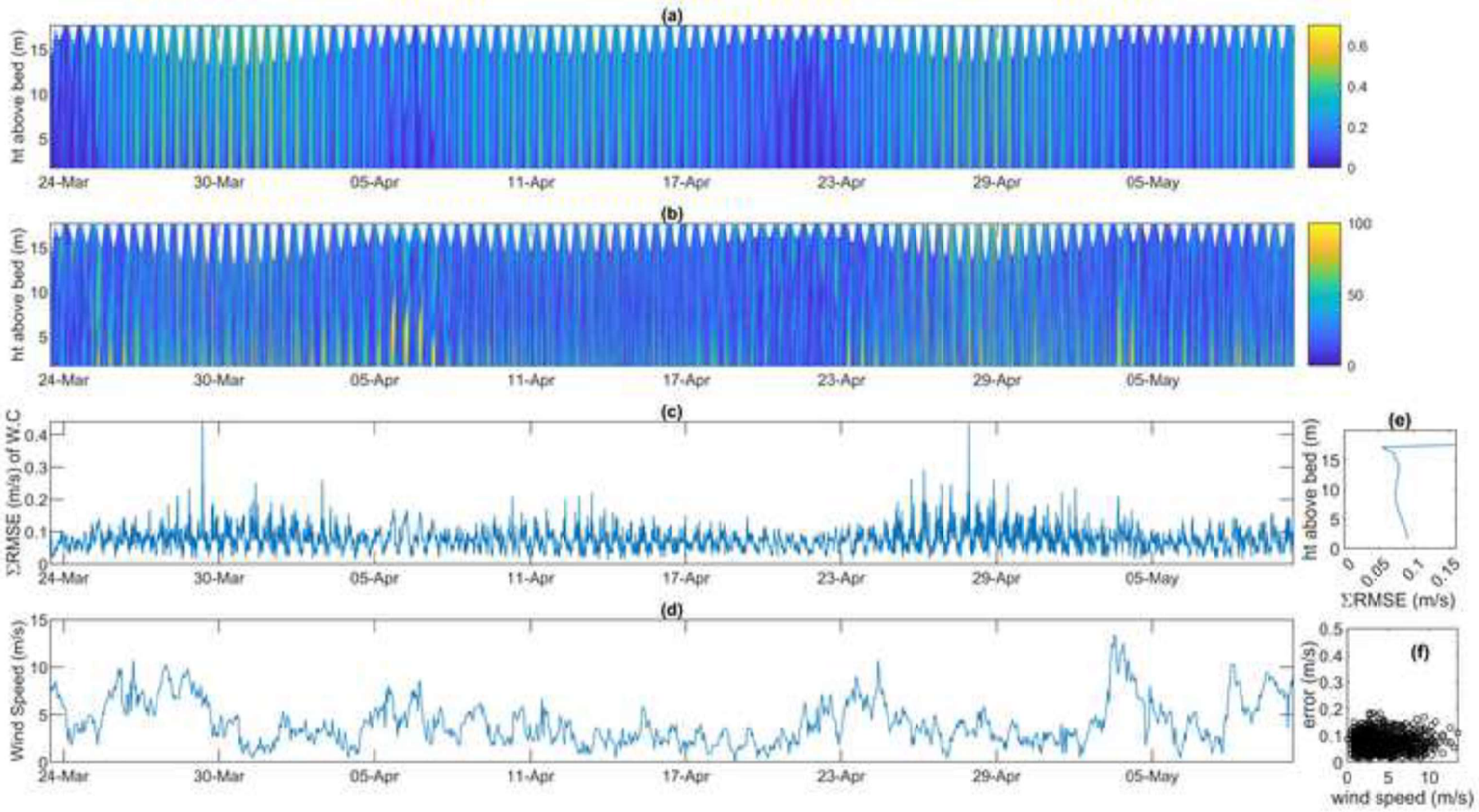

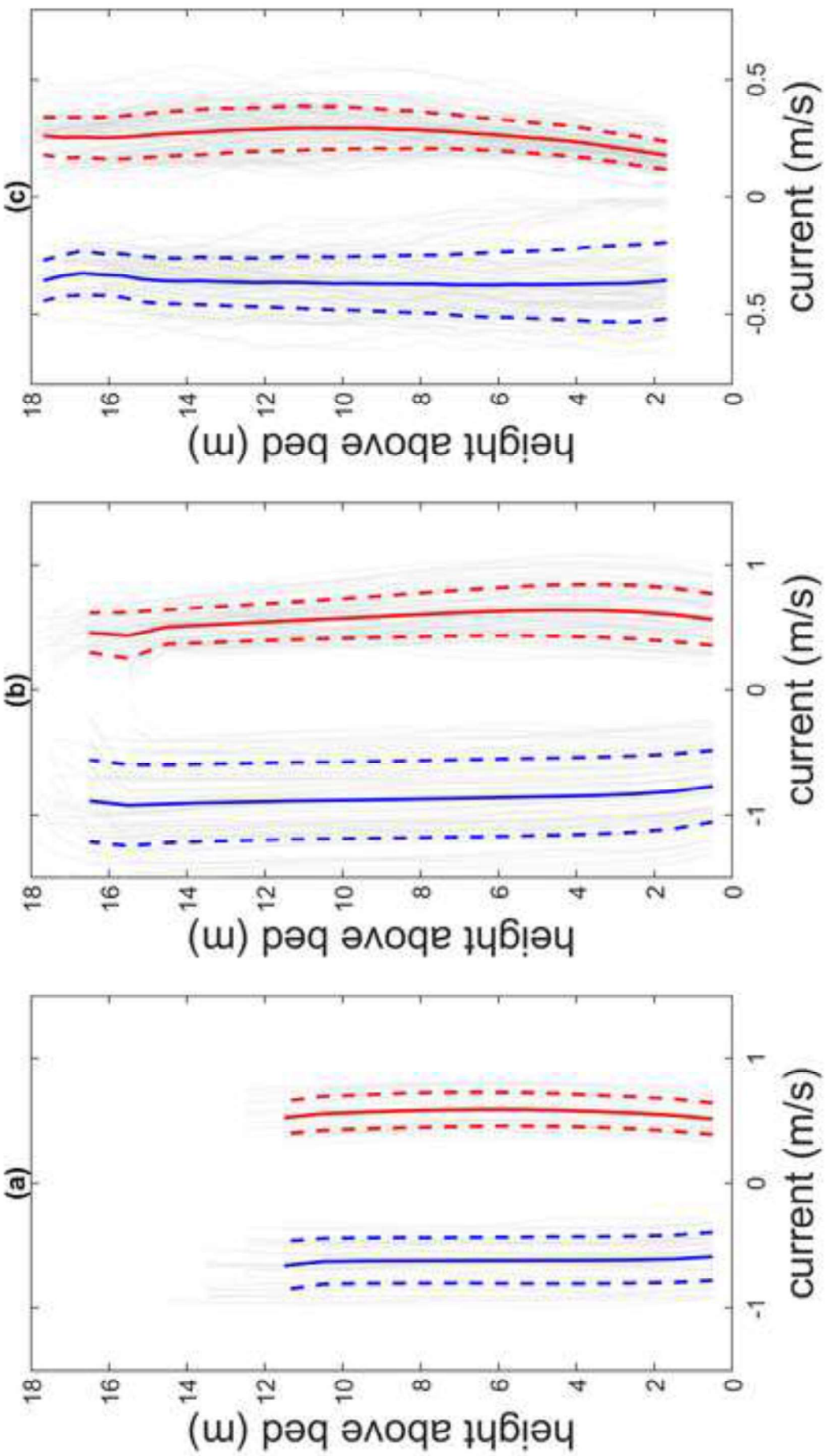

Fig 13

Fig 14

Click here to access/download;Figure;Fig14.png

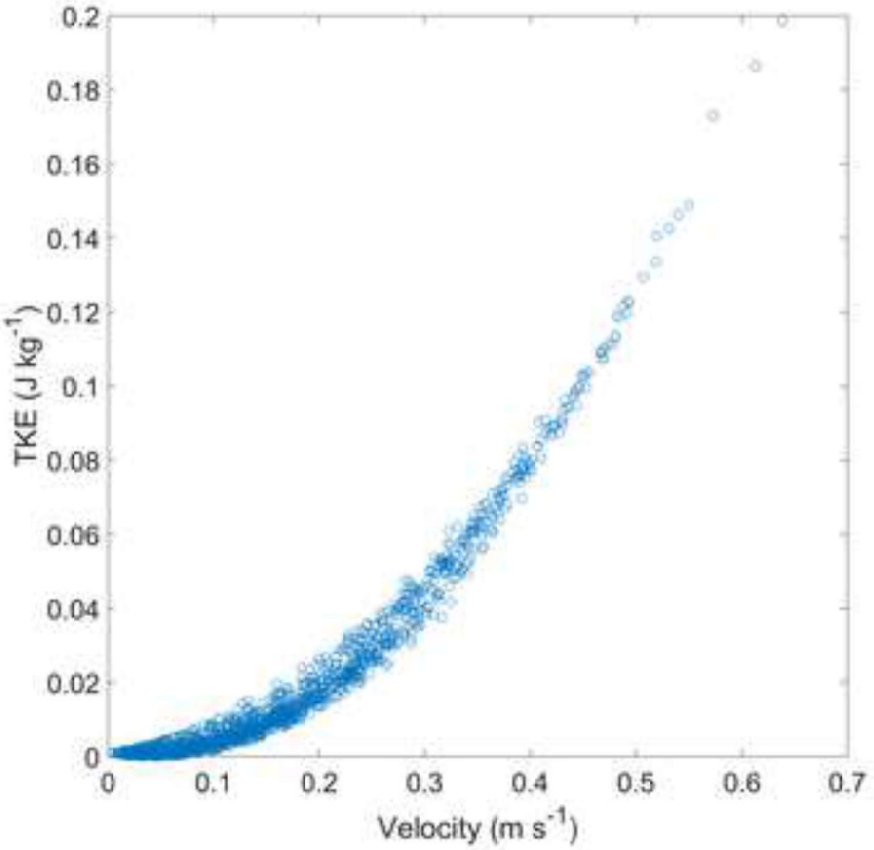

Fig 15

Click here to access/download;Figure;Fig15.png

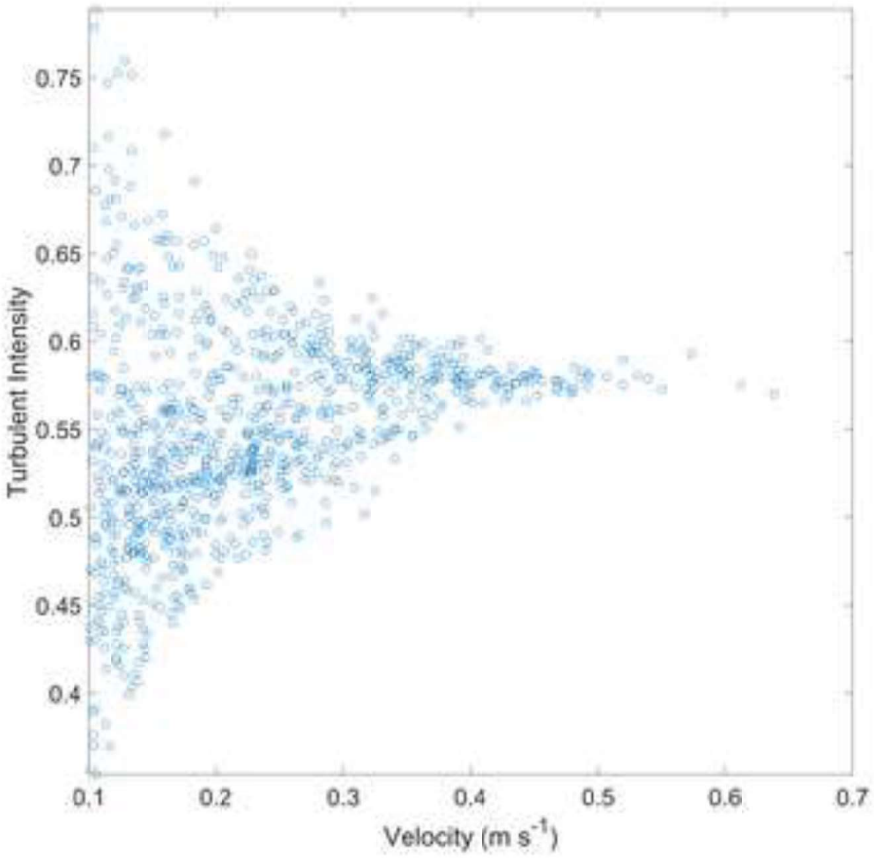

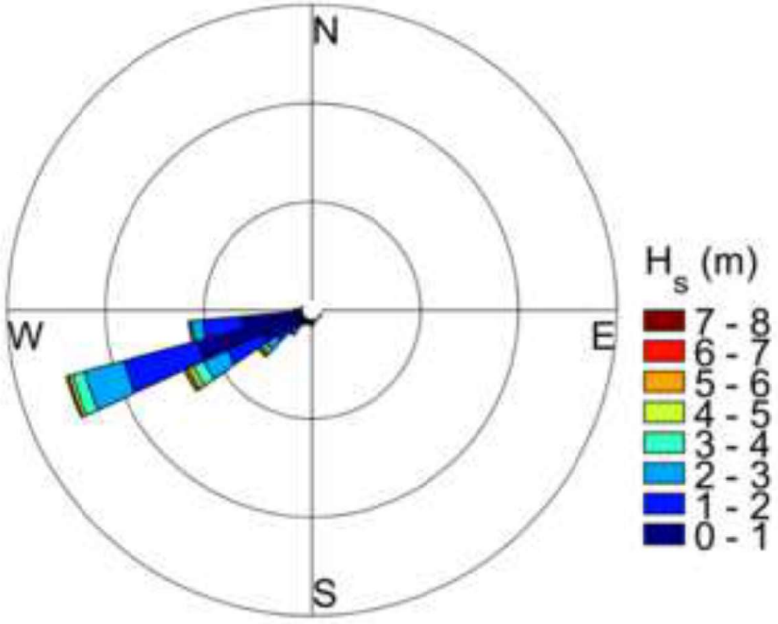

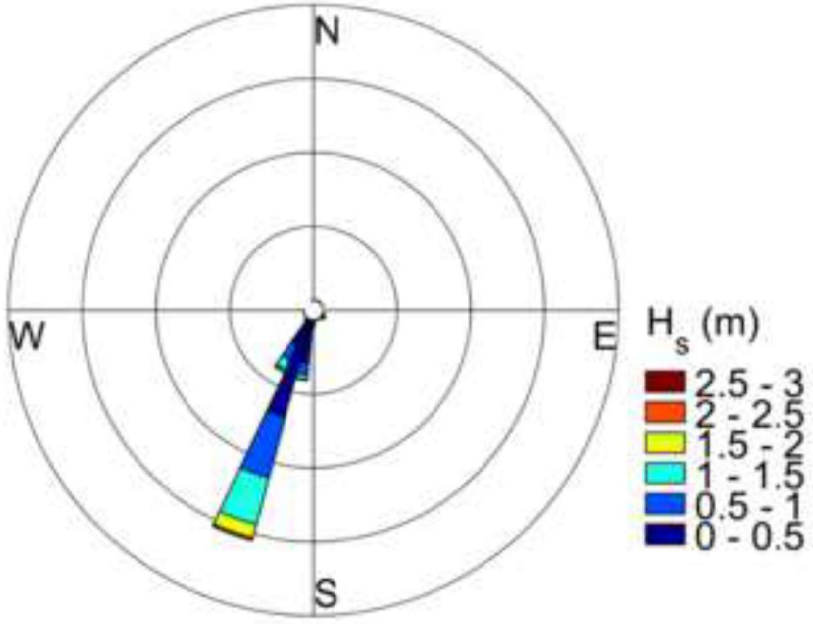

Fig 17

Click here to access/download;Figure;Fig17.png

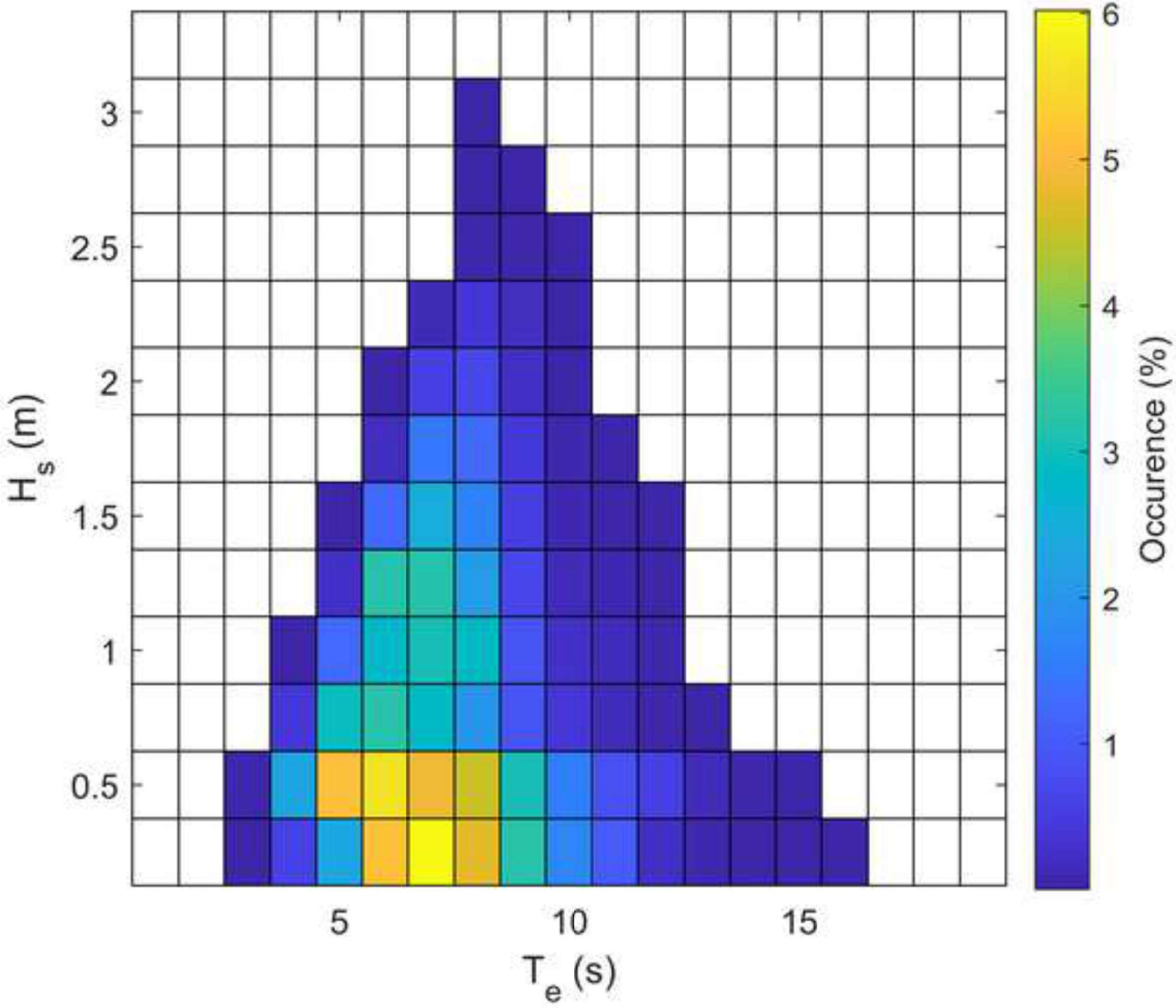

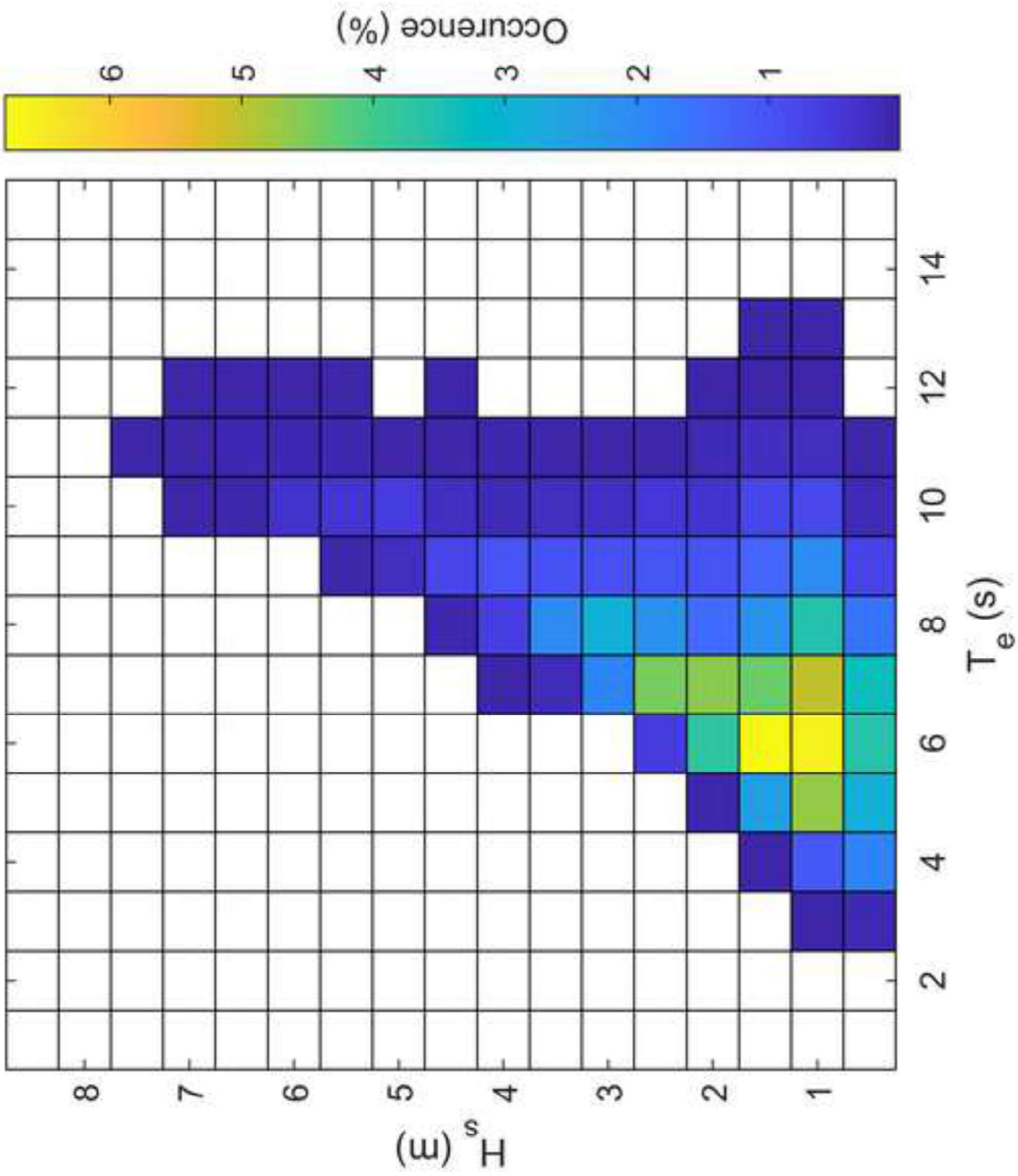

Fig 18

Fig 19

Click here to access/download;Figure;Fig19.png

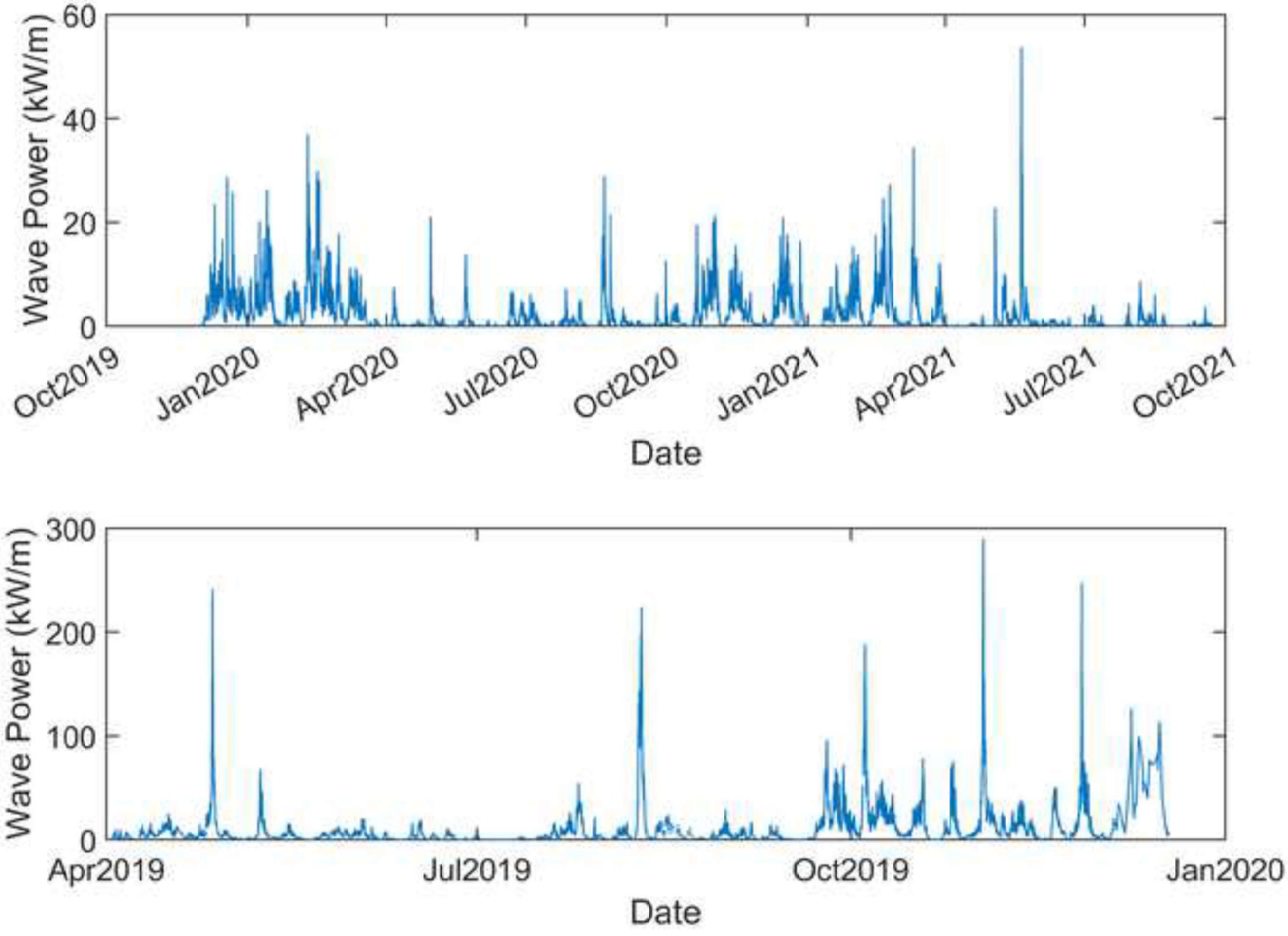

Fig 20

Click here to access/download;Figure;Fig20.png